

การพัฒนาวิธีตรวจวัดกรดแอสคอร์บิก โดพามีนและกรดยูริกโดยใช้ชีวไฟฟ้าคาร์บอนพิมพ์สกรีน  
ดัดแปรด้วยวัสดุระดับนาโนเมตร



นางสาวกาญจนา คุณพาทิ

จุฬาลงกรณ์มหาวิทยาลัย

CHULALONGKORN UNIVERSITY

บทคัดย่อและแฟ้มข้อมูลฉบับเต็มของวิทยานิพนธ์ตั้งแต่ปีการศึกษา 2554 ที่ให้บริการในคลังปัญญาจุฬาฯ (CUIR)  
เป็นแฟ้มข้อมูลของนิสิตเจ้าของวิทยานิพนธ์ ที่ส่งผ่านทางบัณฑิตวิทยาลัย

The abstract and full text of theses from the academic year 2011 in Chulalongkorn University Intellectual Repository (CUIR)  
are the thesis authors' files submitted through the University Graduate School.

วิทยานิพนธ์นี้เป็นส่วนหนึ่งของการศึกษาตามหลักสูตรปริญญาวิทยาศาสตรมหาบัณฑิต

สาขาวิชาเคมี ภาควิชาเคมี

คณะวิทยาศาสตร์ จุฬาลงกรณ์มหาวิทยาลัย

ปีการศึกษา 2558

ลิขสิทธิ์ของจุฬาลงกรณ์มหาวิทยาลัย

Method development for determination of ascorbic acid, dopamine and uric acid  
using nanomaterial-modified screen-printed carbon electrode

Miss Kanjana Kunpatee



A Thesis Submitted in Partial Fulfillment of the Requirements  
for the Degree of Master of Science Program in Chemistry

Department of Chemistry

Faculty of Science

Chulalongkorn University

Academic Year 2015

Copyright of Chulalongkorn University



กาญจนา คุณพาที : การพัฒนาวิธีตรวจวัดกรดแอสคอร์บิก โดพามีนและกรดยูริกโดยใช้  
 ขั้วไฟฟ้าคาร์บอนพิมพ์สกรีนดัดแปรด้วยวัสดุระดับนาโนเมตร (Method development  
 for determination of ascorbic acid, dopamine and uric acid using  
 nanomaterial-modified screen-printed carbon electrode) อ.ที่ปรึกษาวิทยานิพนธ์  
 หลัก: ผศ. ดร.สุชาดา จูอนุวัฒน์กุล, 72 หน้า.

งานวิจัยนี้ได้พัฒนาวิธีตรวจวัดกรดแอสคอร์บิก โดพามีน และกรดยูริกในคราวเดียวกันโดย  
 ใช้ขั้วไฟฟ้าคาร์บอนพิมพ์สกรีนดัดแปรด้วยแกรฟีนควอนตัมดอตและไอออนิกลิควิด แกรฟีนควอนตัม  
 ดอตสังเคราะห์ด้วยวิธีของ Chen และพิสูจน์เอกลักษณ์ด้วยเทคนิคยูวี-วิสิเบิลสเปกโทรสโกปี ฟลูออ  
 เรสเซนซ์สเปกโทรสโกปี และจุลทรรศน์ศาสตร์อิเล็กตรอนชนิดส่องผ่าน ศึกษาการทำงานเชิง  
 เคมีไฟฟ้าของเซนเซอร์โดยใช้ไซคลิกโวลแทมเมตรีและดิฟเฟอเรนเชียลสแควร์โวลแทมเมตรี จากนั้นได้  
 ศึกษาภาวะที่เหมาะสมต่อการตรวจวัดกรดแอสคอร์บิก โดพามีน และกรดยูริกด้วยขั้วไฟฟ้าที่  
 พัฒนาขึ้น พบว่าที่ภาวะเหมาะสมนี้พีคออกซิเดชันของกรดแอสคอร์บิก โดพามีน และกรดยูริก  
 แยกกันอย่างชัดเจน แสดงว่าขั้วไฟฟ้าที่พัฒนาขึ้นสามารถทำให้พีคออกซิเดชันของกรดแอสคอร์บิก โด  
 พามีน และกรดยูริกมีกระแสเพิ่มขึ้นและศักย์ไฟฟ้าลดลง จากนั้นได้ประเมินลักษณะเฉพาะของวิธี  
 วิเคราะห์ที่พัฒนาขึ้น พบว่าการตรวจวัดเชิงเส้นตรงของกรดแอสคอร์บิก โดพามีน และกรดยูริกอยู่  
 ในช่วง 25-400, 0.2-10 และ 0.5-20 ไมโครโมลาร์ และมีขีดจำกัดต่ำสุดของการตรวจวัด 6.64, 0.06  
 และ 0.03 ไมโครโมลาร์ ตามลำดับ นอกจากนี้ยังได้ศึกษาตัวรบกวนที่มีต่อความจำเพาะของ  
 เซนเซอร์ ค่าเบี่ยงเบนมาตรฐานสัมพัทธ์ในการตรวจวัดกระแสของกรดแอสคอร์บิก โดพามีน และ  
 กรดยูริกมีค่าเท่ากับ 4.15, 3.38 และ 3.47 เปอร์เซ็นต์ ซึ่งแสดงให้เห็นว่าขั้วไฟฟ้าที่พัฒนาขึ้นมีการวัด  
 ค่าที่ดี วิธีที่พัฒนาขึ้นนี้สามารถนำไปใช้ตรวจวัดปริมาณกรดแอสคอร์บิกและโดพามีนในตัวอย่าง  
 ยา โดยมีค่าความคลาดเคลื่อนน้อยกว่า 5 เปอร์เซ็นต์ นอกจากนี้ยังสามารถนำมาใช้วิเคราะห์ตัวอย่าง  
 ซีรัมของมนุษย์ด้วยวิธีเดิมสารมาตรฐาน ซึ่งได้ค่าการคืนกลับเป็นที่น่าพอใจ (99 – 107 เปอร์เซ็นต์)

ภาควิชา เคมี

ลายมือชื่อนิสิต .....

สาขาวิชา เคมี

ลายมือชื่อ อ.ที่ปรึกษาหลัก .....

ปีการศึกษา 2558

# # 5671912023 : MAJOR CHEMISTRY

KEYWORDS: GRAPHENE QUANTUM DOTS / IONIC LIQUID / SCREEN-PRINTED ELECTRODE / ASCORBIC ACID / DOPAMINE / URIC ACID

KANJANA KUNPATEE: Method development for determination of ascorbic acid, dopamine and uric acid using nanomaterial-modified screen-printed carbon electrode. ADVISOR: ASST. PROF. SUCHADA CHUANUWATANAKUL, Ph.D., 72 pp.

A novel electrochemical sensor was developed for the simultaneous determination of ascorbic acid (AA), dopamine (DA) and uric acid (UA) using graphene quantum dots and ionic liquid modified screen printed carbon electrode (GQDs/IL-SPCE). GQDs were synthesized via Chen's method and were characterized by UV-vis spectrophotometry, fluorescence spectrophotometry, and transmission electron microscopy (TEM). Cyclic voltammetry (CV) and differential pulse voltammetry (DPV) were employed to study the electrochemical performance of the sensor. The optimum parameters for the determination of AA, DA and UA with GQDs/IL-SPCE were investigated. Well-defined oxidation peaks of the AA, DA and UA were completely separated exhibiting that GQDs/IL modifier provided excellent electrochemical catalytic activity for the oxidation of AA, DA and UA. The linear response ranges for AA, DA and UA were 25-400, 0.2-10 and 0.5-20  $\mu\text{M}$  with detection limit of 6.64, 0.06 and 0.03  $\mu\text{M}$ , respectively. The influence of various interferences on the selectivity of the sensor was studied. The relative standard deviations (RSD) in peak currents of AA, DA and UA were found to be 4.15%, 3.38% and 3.47%, respectively, indicating that the modified electrode had good reproducibility. The proposed method was applied to determine the amount of AA and DA in intravenous drugs with the relative error less than 5%. In addition, the satisfactory result of the sensor has been assessed in human serum sample with good recoveries (99 - 107%) using standard addition method.

Department: Chemistry

Student's Signature .....

Field of Study: Chemistry

Advisor's Signature .....

Academic Year: 2015

## ACKNOWLEDGEMENTS

First of all, I would like to express my sincere thanks and appreciation to my advisor, Asst. Prof. Dr. Suchada Chuanuwatanakul for her kind supervision, invaluable guidance, suggestions and continuous encouragement throughout my Master's Degree study at Chulalongkorn University. I am also cordially thankful to Prof. Dr. Orawon Chailapakul, for her kind advice and encouragement. In addition, I would like to thank Assoc. Prof. Dr. Vudhichai Parasuk from the Department of Chemistry, Faculty of Science, Chulalongkorn University and Dr. Wanida Wonsawat from the Department of Chemistry, Faculty of Science and Technology, Suan Sunandha Rajabhat University, my thesis committee members, for giving valuable comments and advices. Moreover, acknowledgements are extended to Dr. Poomrat Rattanarat, Dr. Eakkasit Punrat, Ms. Prasongporn Ruengpirasiri and all members of the Electrochemistry and Optical Spectroscopy Research Unit for their helpful and comments during the research work.

The author would like to acknowledge the financial support from the 90th Anniversary of Chulalongkorn University Fund (Ratchadaphiseksomphot Endowment Fund), Thailand Research Fund through Research Team Promotion Grant (RTA5780005) and the Electrochemistry and Optical Spectroscopy Research Unit, Department of Chemistry, Faculty of Science, Chulalongkorn University. Thanks also to Department of Chemistry, Faculty of Science, Chulalongkorn University for supporting the facilities which enable this work to be carried out.

Finally, I would like to express my deeply gratitude to my parents and my family for their generous support, tender love, continual care, and invaluable encouragement during study in the M. Sc. program. My special thanks are extended to everyone who helped me to succeed in this dissertation, both during and before my time at Chulalongkorn University.

## CONTENTS

	Page
THAI ABSTRACT .....	iv
ENGLISH ABSTRACT .....	v
ACKNOWLEDGEMENTS .....	vi
CONTENTS .....	vii
LIST OF TABLES .....	xii
LIST OF FIGURES .....	xiv
LIST OF ABBREVIATIONS .....	xx
CHAPTER I INTRODUCTION.....	1
1.1 Introduction .....	1
1.2 Objective of the research.....	3
CHAPTER II THEORY AND LITERATURE SURVEY.....	4
2.1 Ascorbic acid.....	4
2.2 Dopamine .....	5
2.3 Uric acid.....	5
2.4 Electrochemical technique.....	6
2.4.1 Voltammetric methods.....	7
2.4.1.1 Cyclic voltammetry.....	7
2.4.1.2 Differential pulse voltammetry.....	8
2.4.2 Electrodes .....	9
2.4.2.1 Screen-printed carbon electrode .....	9
2.4.2.2 Graphene Quantum dots.....	10
2.4.2.3 Ionic liquid.....	11

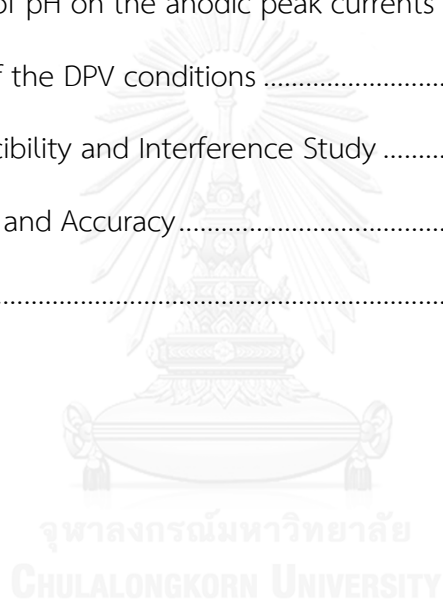
	Page
2.5 Literature reviews .....	12
CHARTER III EXPERIMENTAL.....	15
3.1 Instruments and apparatus.....	15
3.1.1 Synthesis of GQDs .....	15
3.1.2 Characterization of the synthesized GQDs.....	15
3.1.3 Fabrication of the graphene quantum dots and ionic liquid modified screen-printed carbon electrode (GQDs/IL-SPCE).....	16
3.1.4 Morphological characterization of the GQDs/IL-SPCE.....	16
3.1.5 Sample preparations.....	17
3.1.6 Electrochemical measurements of AA, DA and UA.....	17
3.2 Chemicals .....	18
3.2.1 GQDs synthesis.....	18
3.2.2 Fabrication of the GQDs/IL-SPCE.....	18
3.2.3 Electrochemical measurements of AA, DA and UA.....	18
3.2.4 Sample preparations.....	19
3.3 Chemical preparations.....	20
3.3.1 Preparation of solution for GQDs synthesis .....	20
3.3.1.1 10 mg/mL of sodium hydroxide solution .....	20
3.3.1.2 1 mg/mL of citric acid solution.....	20
3.3.2 Preparation of solutions for the determination of AA, DA and UA.....	20
3.3.2.1 0.1 M potassium phosphate monobasic solution.....	20
3.3.2.2 0.1 M potassium phosphate dibasic solution .....	20
3.3.2.3 0.1 M phosphate buffer solution (PBS).....	20



	Page
3.3.2.4 10 mM AA solution .....	21
3.3.2.5 1 mM DA solution .....	21
3.3.2.6 1 mM UA solution.....	21
3.4 Synthesis of GQDs.....	21
3.5 Characterization of GQDs .....	22
3.6 Fabrication of the electrochemical sensors.....	22
3.7 Electrochemical experiments.....	24
3.8 Electrode characterization .....	25
3.9 Optimization of modified electrode .....	25
3.9.1 The amount of IL.....	25
3.9.2 The volume of GQDs .....	25
3.9.3 The effect of electrode pretreatment condition.....	25
3.9.3.1 Pretreatment potential.....	25
3.9.3.2 Pretreatment time .....	26
3.9.4 The effect of scan rate.....	26
3.9.5 The influence of pH on the anodic peak currents of AA, DA and UA.....	26
3.10 Optimization of the DPV parameter.....	26
3.11 Analytical performance.....	27
3.11.1 Linearity, LOD and LOQ .....	27
3.11.2 Reproducibility .....	27
3.11.3 Interference study.....	28
3.12 Real sample analysis .....	28
3.12.1 Determination of AA in Vitamin C tablets.....	28

	Page
3.12.2 Determination of DA in DA injection .....	28
3.12.3 Determination of AA, DA and UA in human serum .....	28
CHAPTER IV RESULTS AND DISCUSSION .....	30
4.1 Characterizations of synthesized GQDs .....	30
4.1.1 UV-Vis and fluorescence spectroscopy .....	30
4.1.2 Transmission electron microscopy .....	31
4.2 Electrochemical characterization of GQDs/IL-SPCE .....	32
4.3 Morphological characterization of the GQDs/IL-SPCE .....	33
4.4 Optimization of modified electrode .....	35
4.4.1 The amount of IL .....	35
4.4.2 The volume of GQDs .....	36
4.4.3 The effect of electrode pretreatment condition .....	37
4.4.3.1 Pretreatment potential .....	37
4.4.3.2 Pretreatment time .....	38
4.4.4 Effect of scan rate .....	39
4.4.5 The influence of pH on the anodic peak currents of AA, DA and UA .....	43
4.5 Optimization of the differential pulse voltammetric conditions .....	45
4.6 Analytical performance .....	48
4.6.1 Linearity, LOD and LOQ .....	48
4.6.2 Reproducibility .....	54
4.6.3 Interference study .....	55
4.7 Real sample analysis .....	56
CHAPTER V CONCLUSIONS AND SUGGESTION FOR FUTURE WORK .....	59

	Page
5.1 Conclusions.....	59
5.2 SUGGESTION FOR FUTURE WORK.....	59
REFERENCES .....	60
APPENDIX.....	65
APPENDIX A Optimization of modified electrode and the DPV conditions.....	66
1. Optimization of modified electrode .....	66
The influence of pH on the anodic peak currents of AA, DA and UA.....	66
2. Optimization of the DPV conditions .....	67
APPENDIX B Reproducibility and Interference Study .....	69
APPENDIX C Precision and Accuracy.....	71
VITA.....	72



## LIST OF TABLES

	<b>Page</b>
<b>Table 3.1</b>	List of instruments and apparatus involved in the synthesis of GQDs..... 15
<b>Table 3.2</b>	List of instruments and apparatus involved in the characterization of the synthesized GQDs..... 16
<b>Table 3.3</b>	List of instruments and apparatus involved in the fabrication of the GQDs/IL-SPCE..... 16
<b>Table 3.4</b>	List of instruments and apparatus involved in the step of sample preparations ..... 17
<b>Table 3.5</b>	Instruments and apparatus for the electrochemical measurements of AA, DA and UA ..... 17
<b>Table 3.6</b>	Information of the chemicals for the GQDs synthesis ..... 18
<b>Table 3.7</b>	List of the chemicals for the fabrication of the GQDs/IL-SPCE ..... 18
<b>Table 3.8</b>	List of the chemicals used for the electrochemical measurements of AA, DA and UA ..... 19
<b>Table 3.9</b>	List of the chemicals in the sample preparations ..... 19
<b>Table 3.10</b>	Preparation of 0.1 M PBS at various pH with the final volume of 100 mL ..... 21
<b>Table 3.11</b>	The optimized parameters for DPV measurement using GQDs/IL-SPCE..... 26
<b>Table 4.1</b>	The optimal DPV parameters for the simultaneous measurement of AA, DA, and UA using GQDs/IL-SPCE..... 48
<b>Table 4.2</b>	The analytical performance of determination of AA, DA, and UA by DPV on the GQDs/IL-SPCE in the presence of the other two species. .... 51

	<b>Page</b>
<b>Table 4.3</b>	The analytical performance of the simultaneous determination of AA, DA and UA by DPV on the GQDs/IL-SPCE..... 54
<b>Table 4.4</b>	Comparison of analytical performance of the simultaneous determination of AA, DA and UA by DPV on the GQDs/IL-SPCE with the other modified electrodes in the literature reports. .... 54
<b>Table 4.5</b>	Determination of ascorbic acid, dopamine and uric acid in vitamin C tablet and dopamine injection (n=3) using our proposed method. .... 57
<b>Table 4.6</b>	Determination of ascorbic acid, dopamine and uric acid in human serum sample (n=3) using our proposed method. .... 58
<b>Table B1</b>	The anodic peak currents of 300 $\mu\text{M}$ AA, 5 $\mu\text{M}$ DA, and 5 $\mu\text{M}$ UA in 0.1 M PBS (pH 4.0) using 5 different sensors..... 69
<b>Table B2</b>	The influences of some metal ions and important biological substances on the peak currents of 100 $\mu\text{M}$ of AA, 10 $\mu\text{M}$ of DA, and 5 $\mu\text{M}$ UA in 0.1 M PBS (pH 4.0). .... 70
<b>Table C1</b>	The acceptable reproducibility, the data from AOAC official method of analysis (2012). .... 71
<b>Table C2</b>	Accuracy consisted from AOAC AOAC official method of analysis (2012). .... 71

## LIST OF FIGURES

	<b>Page</b>
<b>Figure 2.1</b>	Chemical structure of AA ..... 4
<b>Figure 2.2</b>	Chemical structure of DA ..... 5
<b>Figure 2.3</b>	Chemical structure of UA ..... 6
<b>Figure 2.4</b>	(a) Wave form of cyclic voltammetry and (b) cyclic voltammogram of reversible reaction ..... 8
<b>Figure 2.5</b>	(a) Wave form and (b) voltammogram of DPV [24] ..... 9
<b>Figure 2.6</b>	Various applications of GQDs. .... 10
<b>Figure 2.7</b>	Various application of IL [26] ..... 11
<b>Figure 3.1</b>	Pattern of reference electrode ..... 23
<b>Figure 3.2</b>	Template of working electrode, counter electrode and connector position ..... 23
<b>Figure 3.3</b>	The In-house screen-printed carbon electrode with three integrated electrodes (WE: working electrode, RE: reference electrode and CE: counter electrode) ..... 24
<b>Figure 4.1</b>	UV-Vis absorption (red line) and FL spectra (blue line) of the synthesized GQDs. Inset: photographs of the GQDs solution taken under visible light (left) and under black light (right). ..... 30
<b>Figure 4.2</b>	TEM image of the synthesized GQDs ..... 31
<b>Figure 4.3</b>	DPV at bare-SPCE, IL-SPCE, GQDs/SPCE and GQDs/IL-SPCE of ternary mixture of 400 $\mu$ M AA, 10 $\mu$ M DA and 10 $\mu$ M UA in 0.1 M PBS (pH 4.0). ..... 32
<b>Figure 4.4</b>	SEM image of bare-SPCE. .... 34
<b>Figure 4.5</b>	SEM image of IL-SPCE. .... 34

	<b>Page</b>
<b>Figure 4.6</b>	SEM image of GQDs/IL-SPCE..... 34
<b>Figure 4.7</b>	Effect of the IL amount on the peak currents of 1 mM AA, 1 mM DA, and 1 mM UA in 0.1 M PBS (pH 7.0) at GQDs/IL-SPCE. Data are shown as the mean $\pm$ SD and are derived from three replicates..... 35
<b>Figure 4.8</b>	Effect of the amount of GQDs solution on the peak currents of 1 mM AA, 1 mM DA and 1 mM UA in 0.1 M PBS (pH 7.0) at GQDs/IL-SPCE. Data are shown as the mean $\pm$ SD and are derived from three replicates. .... 36
<b>Figure 4.9</b>	Effect of the pretreatment potential on the peak currents of 1 mM AA, 1 mM DA and 1 mM UA in 0.1 M PBS (pH 7.0) at GQDs/IL-SPCE. Data are shown as the mean $\pm$ SD and are derived from three replicates. .... 37
<b>Figure 4.10</b>	Effect of pretreatment potential at 1.7 V and 1.8 V on the DPV responses of 1 mM AA, 1 mM DA and 1 mM UA in 0.1 M PBS (pH 7.0) at GQDs/IL-SPCE..... 38
<b>Figure 4.11</b>	Effect of the pretreatment time on the peak currents of 1 mM AA, 1 mM DA and 1 mM UA in 0.1 M PBS (pH 7.0) at GQDs/IL-SPCE. Data are shown as the mean $\pm$ SD and are derived from three replicates. .... 39
<b>Figure 4.12</b>	Cyclic voltammograms of 1 mM AA in 0.1 M PBS (pH 4.0) on GQDs/IL-SPCE at different scan rates of 10, 20, 30, 40, 50, 60, and 70 mV/s. .... 40
<b>Figure 4.13</b>	Cyclic voltammograms of 1 mM DA in 0.1 M PBS (pH 4.0) on GQDs/IL-SPCE at different scan rates of 10, 20, 30, 40, 50, 60, and 70 mV/s. .... 40

	<b>Page</b>
<b>Figure 4.14</b>	Cyclic voltammograms of 1 mM UA in 0.1 M PBS (pH 4.0) on GQDs/IL-SPCE at different scan rates of 10, 20, 30, 40, 50, 60, and 70 mV/s. .... 41
<b>Figure 4.15</b>	Plots of anodic peak currents of AA vs. square root of scan rates. Data are shown as the mean $\pm$ SD and are derived from three replicates. .... 41
<b>Figure 4.16</b>	Plots of anodic and cathodic peak currents of DA vs. square root of scan rates. Data are shown as the mean $\pm$ SD and are derived from three replicates. .... 42
<b>Figure 4.17</b>	Plots of anodic peak currents of UA vs. square root of scan rates. Data are shown as the mean $\pm$ SD and are derived from three replicates. .... 42
<b>Figure 4.18</b>	Effect of pH on the DPV peak potentials of 1 mM AA, 5 $\mu$ M DA and 10 $\mu$ M UA in 0.1 M PBS at GQDs/IL-SPCE. Data are shown as the mean $\pm$ SD and are derived from three replicates. .... 44
<b>Figure 4.19</b>	Effect of pH on the DPV peak currents of 1 mM AA, 5 $\mu$ M DA and 10 $\mu$ M UA in 0.1 M PBS at GQDs/IL-SPCE. Data are shown as the mean $\pm$ SD and are derived from three replicates. .... 44
<b>Figure 4.20</b>	Effect of step potential on the DPV peak currents of 1 mM of AA, 5 $\mu$ M of DA, and 10 $\mu$ M of UA in 0.1 M PBS (pH 4.0) at GQDs/IL-SPCE. Data are shown as the mean $\pm$ SD and are derived from three replicates. .... 45
<b>Figure 4.21</b>	Effect of pulse amplitude on the DPV peak currents of 1 mM of AA, 5 $\mu$ M of DA, and 10 $\mu$ M of UA in 0.1 M PBS (pH 4.0) at GQDs/IL-SPCE. Data are shown as the mean $\pm$ SD and are derived from three replicates. .... 46



<b>Figure 4.22</b>	Effect of pulse width on the DPV peak currents of 1 mM of AA, 5 $\mu$ M of DA, and 10 $\mu$ M of UA in 0.1 M PBS (pH 4.0) at GQDs/IL-SPCE. Data are shown as the mean $\pm$ SD and are derived from three replicates.....	47
<b>Figure 4.23</b>	Effect of pulse time on the DPV peak currents of 1 mM of AA, 5 $\mu$ M of DA, and 10 $\mu$ M of UA in 0.1 M PBS (pH 4.0) at GQDs/IL-SPCE. Data are shown as the mean $\pm$ SD and are derived from three replicates.....	48
<b>Figure 4.24</b>	DPV AA in the concentration range of 25-400 $\mu$ M in the presence of 1 $\mu$ M DA and 5 $\mu$ M UA. Inset: Calibration curve of AA by DPV using GQDs/IL-SPCE in the presence of DA and UA. Data are shown as the mean $\pm$ SD and are derived from three replicates.....	49
<b>Figure 4.25</b>	DPV of DA in the concentration range of 0.2-15 $\mu$ M in the presence of 0.1 mM AA and 5 $\mu$ M UA. Inset: Calibration curve of DA by DPV using GQDs/IL-SPCE in the presence of AA and UA. Data are shown as the mean $\pm$ SD and are derived from three replicates.....	50
<b>Figure 4.26</b>	DPV of UA in the concentration range of 0.5-20 $\mu$ M in the presence of 0.1 mM AA and 1 $\mu$ M DA. Inset: Calibration curve of UA by DPV using GQDs/IL-SPCE in.....	50
<b>Figure 4.27</b>	DPV of the simultaneous determination of AA (25-400 $\mu$ M), DA (0.2-6 $\mu$ M) and UA (0.5-10 $\mu$ M) in 0.1 M PBS (pH 4.0) using GQDs/IL-SPCE.....	52
<b>Figure 4.28</b>	The calibration curve for the simultaneous determination of AA over the concentration range of 25-400 $\mu$ M in 0.1 M PBS (pH 4.0) by DPV using GQDs/IL-SPCE. Data are shown as the mean $\pm$ SD and are derived from three replicates.....	52

<b>Figure 4.29</b>	The calibration curve for the simultaneous determination of DA over the concentration range of 0.2-6 $\mu\text{M}$ in 0.1 M PBS (pH 4.0) by DPV using GQDs/IL/SPCE. Data are shown as the mean $\pm$ SD and are derived from three replicates. ....	53
<b>Figure 4.30</b>	The calibration curve for the simultaneous determination of UA over the concentration range of 0.5-10 $\mu\text{M}$ in 0.1 M PBS (pH 4.0) by DPV using GQDs/IL-SPCE. Data are shown as the mean $\pm$ SD and are derived from three replicates.....	53
<b>Figure 4.31</b>	Reproducibility results for DPV determination of 300 $\mu\text{M}$ of AA, 10 $\mu\text{M}$ of DA and 5 $\mu\text{M}$ of UA in 0.1 M PBS (pH 4.0) using 5 different sensors. ....	55
<b>Figure 4.32</b>	Effect of various foreign substances at 1000 $\mu\text{M}$ on the simultaneous determination of 100 $\mu\text{M}$ of AA, 10 $\mu\text{M}$ of DA, and 5 $\mu\text{M}$ UA in 0.1 M PBS (pH 4.0) by DPV at GQDs/IL-SPCE. Data are shown as the mean $\pm$ SD and are derived from three replicates.....	56
<b>Figure 4.33</b>	The DPV responses of human serum sample containing different concentrations of added AA, DA and UA in 0.1 M PBS (pH 4.0) on the GQDs/IL-SPCE. Concentration of added three compounds: AA (0, 50, 100, 150, 200 $\mu\text{M}$ ), DA (0, 1, 2, 3, 4 $\mu\text{M}$ ), UA (0, 2, 4, 6, 8 $\mu\text{M}$ ).....	58
<b>Figure A1</b>	Effect of pH on the DPV responses of 1 mM AA, 5 $\mu\text{M}$ DA and 10 $\mu\text{M}$ UA in 0.1 M PBS (pH 4.0) at GQDs/IL-SPCE. ....	66
<b>Figure A2</b>	Effect of step potential on the DPV responses of 1 mM AA, 5 $\mu\text{M}$ DA and 10 $\mu\text{M}$ UA in 0.1 M PBS (pH 4.0) at GQDs/IL-SPCE.....	67
<b>Figure A3</b>	Effect of pulse amplitude on the DPV responses of 1 mM AA, 5 $\mu\text{M}$ DA and 10 $\mu\text{M}$ UA in 0.1 M PBS (pH 4.0) at GQDs/IL-SPCE.....	67

<b>Figure A4</b>	Effect of pulse width on the DPV responses of 1 mM AA, 5 $\mu$ M DA and 10 $\mu$ M UA in 0.1 M PBS (pH 4.0) at GQDs/IL-SPCE.....	68
<b>Figure A5</b>	Effect of pulse time on the DPV responses of 1 mM AA, 5 $\mu$ M DA and 10 $\mu$ M UA in 0.1 M PBS (pH 4.0) at GQDs/IL-SPCE.....	68



## LIST OF ABBREVIATIONS

A	ampere
AA	ascorbic acid
CV	cyclic voltammetry
DA	dopamine
DPV	differential pulse voltammetry/differential pulse voltammogram
E	potential
FL	fluorescence spectroscopy
GQDs	graphene quantum dots
IL	liquid ionic
L	liter
LOD	limit of detection
LOQ	limit of quantification
mg	milligram
mL	milliliter
mV	millivolt
PBS	phosphate buffer solution
PVC	polyvinyl chloride
RSD	relative standard deviation
SEM	scanning electron microscope
SD	standard deviation
SPCE	screen-printed carbon electrode

TEM	transmission electron microscopy
UA	uric acid
UV-Vis	ultraviolet-visible
V	volt
$\mu\text{g}$	microgram
$\mu\text{L}$	microliter
$^{\circ}\text{C}$	degree Celsius



# CHARTER I

## INTRODUCTION

### 1.1 Introduction

Ascorbic acid (AA), dopamine (DA) and uric acid (UA) are important biological molecules for physiological process in human metabolism, coexisting in the normal human serum and extra cellular fluids of central nervous system. Ascorbic acid (vitamin C) is essential component in human diet, which is a very popular antioxidant property. It can be found in many biological systems and various samples such as fresh vegetables and fruits, pharmaceutical and cosmetic products [1]. AA is commonly used to prevent and treat common cold, mental illnesses and cancers [2]. Next, DA is the catecholamine neurotransmitter which plays important roles in control of central nervous system. Abnormal levels of DA may lead to cause various neurological diseases such as Parkinson and schizophrenia [3]. Moreover, DA is able to be used as an intravenous medication which acts on the sympathetic nervous system to produce effects, corresponding to increase heart rate and blood pressure [4]. Then, UA is the main primary final product of purine metabolism. High UA concentration leads to occur some diseases, such as gout, hyperuricaemia, high blood pressure and kidney disease [5]. Therefore, the determination of these biomarkers is important for investigating their physiological functions and clinical diseases diagnosis.

Many conventional analytical methods are employed for the detection of these analytes of interest such as capillary electrophoresis, fluorometry, liquid chromatography-tandem mass spectrometry (LC-MS/MS) and chemiluminescence spectroscopy [6-9]. These conventional methods have advantage of high selectivity, sensitivity and efficiency for the determination of these biomolecules. However, the main limitations of these methods are time-consumption, complicated instrument, required trained personal, expensiveness and unsuitable for on-site analysis.

Electrochemical method has attracted much interest for determination of AA, DA and UA because of their high sensitivity, short-time analysis, low cost and more suitability for the simultaneous detection of these biomarkers due to their electroactive nature. On the other hand, there is a major problem for electrochemical detection of AA, DA and UA which these compounds are oxidized at the same standard potential, resulting that overlapping of the oxidation peak of these three species at traditional electrodes or unmodified electrode was observed.

Several modified electrodes were developed to resolve of this problem. Various outstanding materials such as polymer [10, 11], noble metal/alloy nanoparticles [12, 13], carbon-based material [14, 15] and ionic liquid [16, 17] were introduced as an electrode modifier. Screen-printed carbon electrode (SPCE) has attracted considerable attention over the traditional electrodes because of simple fabrication, mass production, low cost, portability, disposability and easy surface modification with various materials [18]. To improve the sensitivity, the SPCE was modified with graphene quantum dots (GQDs) and ionic liquid (IL). GQDs are graphene sheets with lateral dimension smaller than 100 nm which have various excellent electronic and optoelectronic properties from quantum confinement and edge effects. Furthermore, the GQDs showed stable luminescence, low toxicity, high conductivity, and good biocompatibility which demonstrated to be appropriate and efficient in both bioimaging and biosensing applications [19, 20]. Ionic liquid is one of interesting materials used to modify electrode surface because it has many unique electrochemical properties such as high thermal stability, high ionic conductivity, wide electrochemical window and biocompatibility. Thus, both materials consisting of GQDs and IL are promising electrode modifier and might be suitable for highly sensitive and selectivity determination of AA, DA and UA [16].

In this work, the graphene quantum dots and ionic liquid modified screen-printed carbon electrode (GQDs/IL-SPCE) is used to perform the sensitive and simultaneous determination of AA, DA and UA. The proposed electrode modifier including GQDs and IL can increase electrode surface and conductivity, leading to improve electrochemical performance of sensor. The GQDs/IL-SPCE has good

sensitivity, selectivity, reproducibility, and low detection limit. The application of the GQDs/IL-SPCE towards the quantification of AA, DA and UA in real samples was found to be promising.

## 1.2 Objective of the research

This research consists of three main goals for development method as follows:

1. To synthesize and characterize graphene quantum dots and use as electrode modifier.
2. To develop the novel method for simultaneous detection of AA, DA and UA using graphene quantum dots and ionic liquid modified screen-printed carbon electrode (GQDs/IL-SPCE).
3. To apply the developed method for the simultaneous determination of AA, DA and UA in real biological and pharmaceutical samples.



## CHAPTER II

### THEORY AND LITERATURE SURVEY

This chapter focuses on detail and the important of AA, DA and UA. The theory of electrochemical method used in this work is explained. The properties of GQDs and IL as the modifier electrode were defined. The literature survey of the current developed method for the determination of these three analytes is presented.

#### 2.1 Ascorbic acid

Ascorbic acid, AA (vitamin C) is a water-soluble ketolactone with two ionizable hydroxyl groups (Figure 2.1). It has two  $pK_a$ ,  $pK_1$  of 4.04 and  $pK_2$  of 11.34 which can occur as an ascorbate anion at physiological condition. AA has a reductive properties which acts as a powerful antioxidant against free-radical. Thus, it also has been used for prevention and treatment of common cold, mental illness, infertility, cancer and AIDS. AA can be found in many biological systems and foodstuffs. In addition, AA is commonly used in large scale as an antioxidant in food, animal feed, pharmaceutical formulations and cosmetic applications [1].

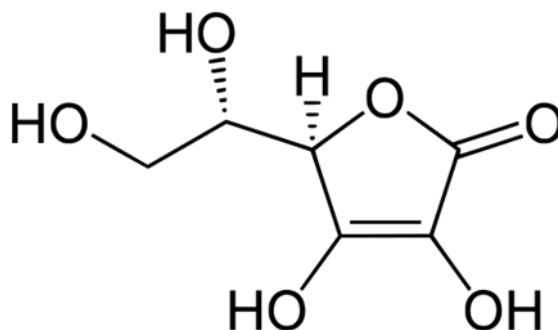


Figure 2.1 Chemical structure of AA

## 2.2 Dopamine

Dopamine, DA (3, 4-dihydroxyphenyl ethylamine) is an important neurotransmitter in the mammalian central nervous, cardiovascular and hormonal systems (see chemical structure in Figure 2.2). It has important role in regulation of cognitive functions such as stress, behavior and attention. In biological system, the normal concentration range of DA is found in the brain at approximately  $50 \text{ nmol g}^{-1}$  and in extracellular fluids at  $10^{-8}$  to  $10^{-6}$  M. Abnormal concentrations of DA is linked to many diseases, for example, parkinsonism, epilepsy and schizophrenia [21].

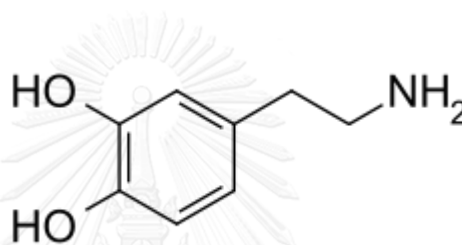
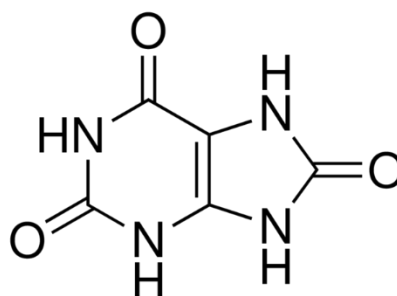


Figure 2.2 Chemical structure of DA

## 2.3 Uric acid

Uric acid, UA (2,6,8-trihydroxypurine), the final product of the inert purine metabolism (see chemical structure in Figure 2.3), is related to many clinical disorders. For a healthy person, the concentration of UA found in the serum is ranging from about 240 to 520  $\mu\text{M}$ , and in the urinary excretion the concentration is ranging from about 1.49 to 4.46  $\text{mM}/24 \text{ h}$ . High concentrations of UA in human body have been linked to many diseases, such as gout, hyperuricaemia, Lesch-Nyan disease, obesity, diabetes, high cholesterol, high blood pressure, kidney disease and heart disease [22].



**Figure 2.3** Chemical structure of UA

For diagnosis of these diseases, the measurements of AA, DA and UA in biological samples are required. As AA, DA and UA are electrochemically active, electrochemical technique is suitable for using as a detection method for these three analytes.

#### 2.4 Electrochemical technique

Electrochemical technique is a technique in analytical chemistry that study the chemical response of a system to an electrical stimulation. The loss of electrons (oxidation) or gain of electrons (reduction) undergoes during the electrical stimulation are commonly known as redox reaction. The reaction can provide information about the reaction mechanisms, kinetics, concentration, chemical status and other behavior of a species in solution. The electrochemical method has many advantages such as high sensitivity, rapid response, simple operation, low expense and suitable for simultaneous determination of various analytes. For the selection of the electrochemical methods, it depended on the character of the compound to be determined and the matrix components of the sample [23]. In this part, voltammetric method which is an electrochemical method used in this work is explained.

### 2.4.1 Voltammetric methods

Voltammetric method is basically referred to as techniques with the common characteristics that the potential is controlled and the monitoring of resulting current flowing through the electrode. The various voltammetric techniques provide many advantages such as excellent sensitivity, a large number of useful solvents as electrolytes, a wide range of temperature, rapid analysis time, simultaneous determination of several analytes, the ability to determine kinetic and mechanistic parameters, etc. This method consists of three electrodes which are working electrode, reference electrode and counter (or auxiliary) electrode. The three electrodes are connected to a potentiostat. The potential is applied between working electrode and reference electrode, and then the current that flows between the working and auxiliary electrode is measured. The resulting plot of current versus applied potential is call voltammogram.

In this research, voltammetric methods, including cyclic voltammetry and differential pulse voltammetry, were used for characterization of modified electrode and determination of AA, DA and UA. These methods will be explained in the following section.

#### 2.4.1.1 Cyclic voltammetry

Cyclic voltammetry (CV) is one of the commonly used electroanalytical techniques, it is widely used for the study of redox processes, for understanding reaction intermediates, and for obtaining stability of reaction products. It is not usually a good technique for quantitative analysis. In the experiment of CV, the potentiostat applies a potential ramp to the working electrode to gradually change potential and then reverses the scan, returning to the initial potential (see Figure 2.4a). During the potential sweep, the potentiostat measures the current resulting from the applied potential. These values are then used to plot the CV graph of current versus the applied potential that is shown in Figure 2.4b.

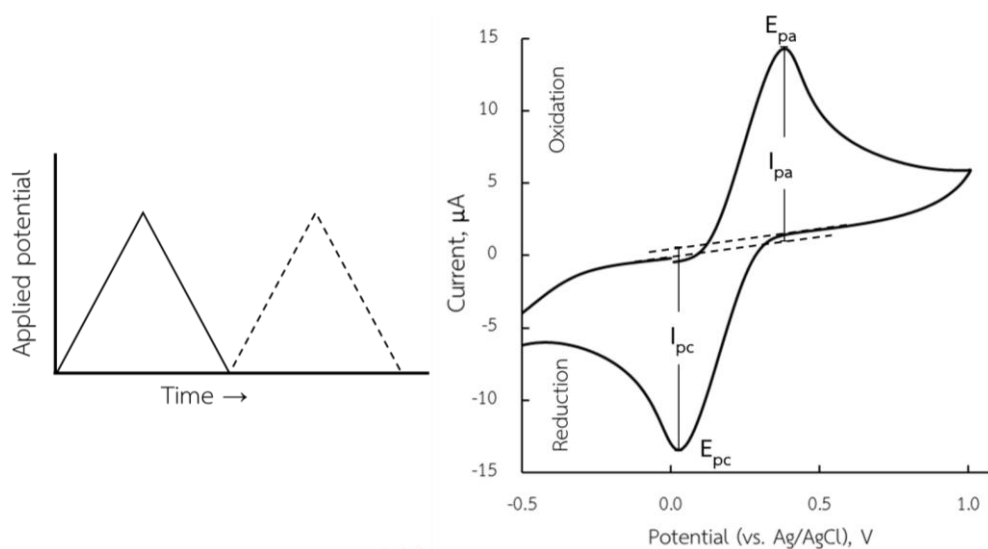


**Figure 2.4** (a) Wave form of cyclic voltammetry and (b) cyclic voltammogram of reversible reaction.

The important parameters in a cyclic voltammogram are the peak potentials ( $E_{pc}$ ,  $E_{pa}$ ) and peak currents ( $i_{pc}$ ,  $i_{pa}$ ) of the cathodic and anodic peaks, respectively.

For a reversible system, the peak height will increase linearly with the square root of the scan rate. The slope of the resulting line will be proportional to the diffusion coefficient, as shown in the Randles-Sevcik equation.

$$i_p = 269n^{3/2}AD^{1/2}\nu^{1/2}C^b$$

Where  $i_p$  is the peak current in ampere,  $A$  is the electrode area ( $\text{cm}^2$ ),  $D$  is the diffusion coefficient ( $\text{cm}^2 \text{s}^{-1}$ ),  $C^b$  is the concentration in  $\text{mol L}^{-1}$ , and  $\nu$  is the scan rate in  $\text{V s}^{-1}$ .

#### 2.4.1.2 Differential pulse voltammetry

Differential pulse voltammetry (DPV) is a part of pulse voltammetry. This technique is scanned with a series of pulses. The DPV potential pulse is fixed and is superimposed on a slowly changing base potential (Figure 2.5a). The current is measured at two points for each pulse, the first point (1) just before

the application of the pulse and the second (2) at the end of the pulse. These sampling points are selected to allow for the decay of the nonfaradaic (charging) current. The difference between current measurements at these points for each pulse is determined and plotted against the base potential that are shown in Figure 2.5b.

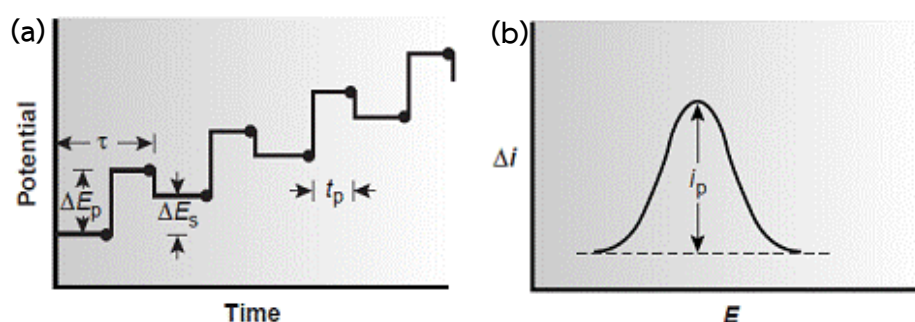


Figure 2.5 (a) Wave form and (b) voltammogram of DPV [24]

## 2.4.2 Electrodes

The voltammetric experiment is performed with three electrodes that consists of a working electrode, a reference electrode and a counter electrode. Normally, the electrode provides the interface across which a charge can be transferred. At the convenient applied potential, the reduction or oxidation of electroactive specie occurs at the surface of a working electrode, results in the mass transport of new material to the electrode surface and the generation of a current.

### 2.4.2.1 Screen-printed carbon electrode

Screen-printed carbon electrode (SPCE) is a disposable electrode that finds a widely use in electrochemical sensor. A SPCE consists of a chemically inert substrate on which three electrodes, the working electrode, the pseudo reference electrode and the counter electrode are printed through screen-printing methodology. On the production of the WE, the most commonly used

materials are carbon ink or different forms of carbon such as graphene, graphite and carbon nanotube. Ag/AgCl is the mostly used material as a pseudo reference electrode and carbon ink was printed as conductive tracks. The SPCE has several advantages such as simple fabrication, mass production, low cost, portability, disposability and easy surface modification with various materials [25]. To improve the sensitivity, the SPCE was modified with GQDs and IL for the simultaneous determination of AA, DA and UA.

### 2.4.2.2 Graphene Quantum dots

Graphene Quantum dots (GQDs) are graphene nanosheets in the form of one, two or more layers all less than 10 nm thick and 100 nm in lateral size. It usually contains functional groups (carboxyl, hydroxyl, carbonyl, epoxide) at their edges that can act as reaction sites and alter emission from the dots by changing their electron density. GQDs have various electronic and optoelectronic properties from quantum confinement and edge effects. Further, the GQDs showed stable luminescence, low toxicity, high conductivity, and good biocompatibility which demonstrated to be efficient in both bioimaging and biosensing applications (Figure 2.6). [19, 20]

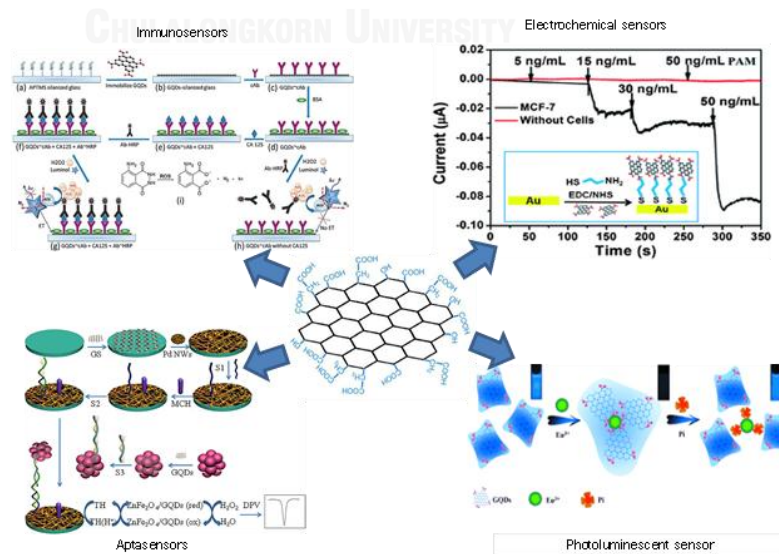


Figure 2.6 Various applications of GQDs.

### 2.4.2.3 Ionic liquid

Ionic liquid (IL) is commonly composed of organic cations and various inorganic anions, which exists in the liquid state at room temperature. IL is one of interesting materials used to modify electrode because it has many unique electrochemical properties such as high thermal stability, high ionic conductivity, wide electrochemical window and biocompatibility. Due to these properties, ILs have received much attention for use in various applications (Figure 2.7). For example, ILs have been proved to be effective modifiers and stabilizers for preparation and functionalization of carbon nanotubes and noble metal nanoparticles. Thus, modification of electrode with IL has been widely investigated for analysis of AA, DA and UA [16, 17].

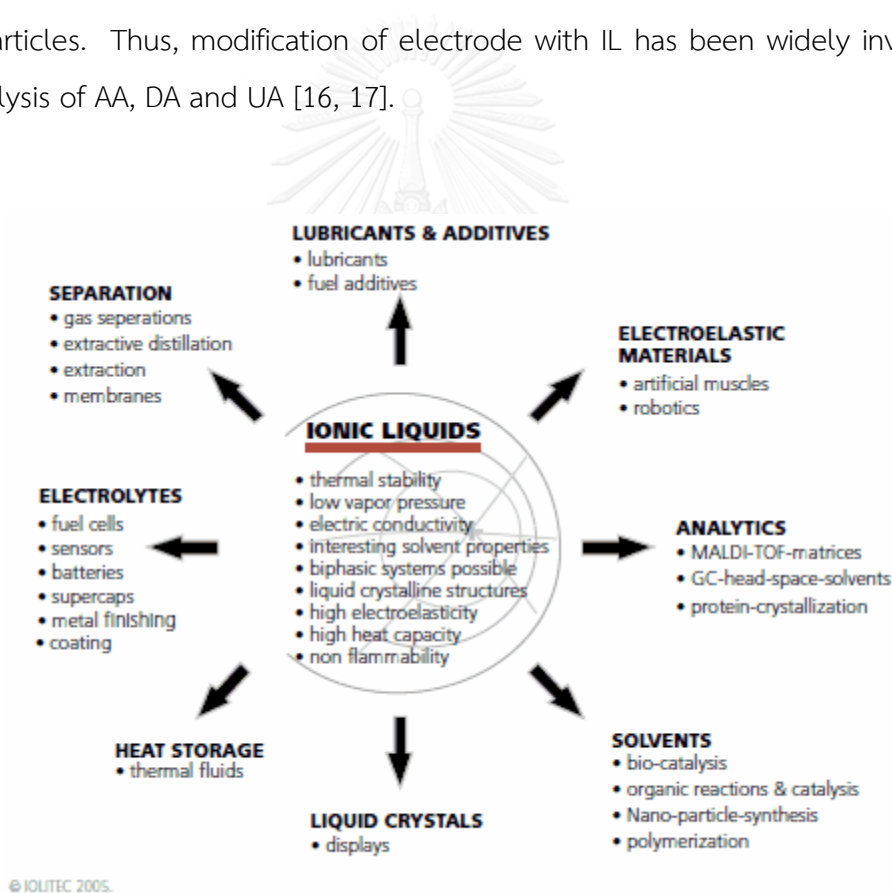


Figure 2.7 Various application of IL [26].



## 2.5 Literature reviews

In 2006, Safavi *et al.* [16] developed the constructed carbon ionic liquid electrode (CILE) for the simultaneous determination of dopamine, ascorbic acid and uric acid. The results show that CILE reduced the overpotential of DA, AA, and UA oxidation, without showing any fouling effect due to the deposition of their oxidized products. In the case of DA, the oxidation and reduction peak potentials appeared at 210 and 135 mV (vs. Ag/AgCl, KCl, 3.0 M), respectively, and the CILE showed a significantly better reversibility for dopamine.

In 2012, Ping *et al.* [17] reported a novel SPE prepared from graphene and ionic liquid doped screen-printing ink for simultaneous determination of AA, DA and UA. In the co-existence system of these three species, the linear response ranges for the determination of AA, DA, and UA were 4.0–4500  $\mu\text{M}$ , 0.5–2000  $\mu\text{M}$ , and 0.8–2500  $\mu\text{M}$ , respectively. The detection limits ( $S/N = 3$ ) were found to be 0.95  $\mu\text{M}$ , 0.12  $\mu\text{M}$ , and 0.20  $\mu\text{M}$  for the determination of AA, DA, and UA, respectively.

In 2012, Dong *et al.* [27] developed an easy bottom-up method for the preparation of photoluminescent (PL) graphene quantum dots (GQDs) and graphene oxide (GO) by tuning the carbonization degree of citric acid and dispersing the carbonized products into alkaline solutions. The GQDs are nanosheets  $\sim 15$  nm in width, and 0.5–2.0 nm in thickness. The GO nanostructures consisted of sheets that were hundreds of nanometers in width and  $\sim 1$  nm in height. They exhibited a relatively weak (2.2%) PL quantum yield and an excitation-dependent PL emission activity.

In 2014, Roushani, M. and Abdi, Z [28] reported a novel and sensitive electrochemical sensor based on graphene quantum dots/riboflavin modified glassy carbon (GC/GQDs/RF) electrode for determination of persulfate ( $\text{S}_2\text{O}_8^{2-}$ ). To activate the surface of GC/GQDs electrode, pre-treatment was performed potentiostatically at 1.7 V.

In 2014, Afraz *et al.* [29] modified a carbon paste electrode (CPE) with multiwalled carbon nanotubes (MWCNTs) and an ionic liquid (IL) for the

simultaneous determination of AA, DA and UA. Three sharp and well-separated oxidation peaks for AA, DA and UA were obtained. The sensor enabled the simultaneous determination of AA, DA and UA with linear responses from 0.3 to 285, 0.08 to 200, and 0.1 to 450  $\mu\text{M}$ , respectively, and with 120, 30 and 30 nM detection limits (at an S/N of 3).

In 2014, Yang *et al.* [30] developed an ERGO film modified electrode via drop-casting of graphene oxide (GO) dispersion on the surface of GCE followed by an electrochemical reduction process. The modified electrode was applied to simultaneously determine AA, DA and UA. DPV results showed that DA, AA and UA could be detected selectively and sensitively at ERGO/GCE with peak-to-peak separation of 240 mV and 130 mV for AA-DA and DA-UA, respectively. The linear ranges for AA, UA and DA were 500–2000  $\mu\text{M}$ , 0.5–60  $\mu\text{M}$  and 0.5–60  $\mu\text{M}$ , respectively.

In 2014, Wang *et al.* [31] reported an electrochemical biosensor for the simultaneous determination of DA and UA in the presence of AA using a glassy carbon electrode modified with 1-butyl-3-methylimidazolium 2-amino-3-mercaptopropionic acid salt ionic liquid functionalized graphene (IL-G/GCE). The separations of oxidation peak potentials of AA-DA, DA-UA, and AA-UA were 147, 145 and 292 mV, respectively.

In 2014, Hu *et al.* [32] developed and characterized a new dopamine (DA) sensor based on the reduced graphene oxide (rGO)-carbon dot composite film. The rGO-CDs electrode (GCE) showed better electrochemical response towards the detection of DA than the bare GCE, GO/GCE and CDs/GCE. A linear relationship between the oxidation peak current of DA and its concentration could be obtained in a range of 0.01000  $\mu\text{M}$  to 450.0  $\mu\text{M}$  with the limit of detection of 1.5 nM (3S/N).

In 2014, Nancy *et al.* [33] reported a development of novel solar graphene-nickel hydroxide modified glassy carbon electrode for the simultaneous detection of AA, DA and UA. The sensor exhibited appreciable electrocatalytic effect for the simultaneous detection of lower concentrations of the analytes compared to solar graphene modified glassy carbon electrode. The detection limits attained by DPV

were 30  $\mu\text{M}$ , 120 nM and 0.46  $\mu\text{M}$  for AA, DA and UA respectively. Recovery values ranging from 98 - 104% were obtained for the analysis of real samples.

In 2015, Zhao *et al.* [34] fabricated electrochemical deposition of MgO nanobelts on a graphene-modified tantalum wire (denoted as MgO/Gr/Ta) electrode for the simultaneous detection of AA, DA and UA. The CV results showed that AA, DA and UA could be detected simultaneously using MgO/Gr/Ta electrode with peak-to-peak separation of 300 mV, 147 mV and 447 mV for AA-DA, DA-UA and AA-UA, respectively. In the threefold co-existence system, the linear calibration plots for AA, DA and UA were obtained over the concentration range of 5.0–350  $\mu\text{M}$ , 0.1–7  $\mu\text{M}$  and 1–70  $\mu\text{M}$  with detection limits of 0.03  $\mu\text{M}$ , 0.15  $\mu\text{M}$  and 0.12  $\mu\text{M}$ , respectively.



## CHARTER III

### EXPERIMENTAL

This chapter provided the information of instruments and apparatus, chemicals and reagents, sample preparations, GQDs synthesis and characterization, preparation of modified electrode, electrode characterization and electrochemical measurement.

#### 3.1 Instruments and apparatus

##### 3.1.1 Synthesis of GQDs

The instruments and apparatus used for the synthesis of GQDs are listed in Table 3.1

**Table 3.1** List of instruments and apparatus involved in the synthesis of GQDs

Instruments and apparatus	Suppliers
Hot plate stirrer, HL HS-115	Harikul Science, Thailand
Magnetic stirring bars	SGS ICS, Switzerland
Universal indicator test paper, pH 1-14	Merck, Germany
Milli-Q ultrapure water purification system (R > 18.2 M $\Omega$ ·cm)	Millipore, USA
Glasswares	

##### 3.1.2 Characterization of the synthesized GQDs

For the characterization of the synthesized GQDs, the instruments and apparatus used are shown in Table 3.2.

**Table 3.2** List of instruments and apparatus involved in the characterization of the synthesized GQDs

Instruments and apparatus	Suppliers
UV-Vis spectrophotometer	Agilent, USA
Cary Eclipse Fluorescence Spectrophotometer	Agilent, USA
Transmission electron microscope	JEOL, USA
Quartz cuvette	
Plastic cuvette	

### 3.1.3 Fabrication of the graphene quantum dots and ionic liquid modified screen-printed carbon electrode (GQDs/IL-SPCE)

The instruments and apparatus used for the fabrication of the GQDs/IL-SPCE are listed in Table 3.3.

**Table 3.3** List of instruments and apparatus involved in the fabrication of the GQDs/IL-SPCE

Instruments and apparatus	Suppliers
Screen-printed blocks	Chaiyaboon, Thailand
Ultrasonic bath, ULTRA Asonik 28H	ESP Chemical, USA
Hot air oven	Memmert, USA
Glasswares	

### 3.1.4 Morphological characterization of the GQDs/IL-SPCE

The surface of GQDs/IL-SPCE is morphologically characterized by using scanning electron microscope (SEM) from JEOL, USA.

### 3.1.5 Sample preparations

The instruments and apparatus for the sample preparations are recorded in Table 3.4.

**Table 3.4** List of instruments and apparatus involved in the step of sample preparations

Instruments and apparatus	Suppliers
pH meter	Metrohm, Switzerland
Micropipette and tips	Eppendorf, Germany
Milli-Q ultrapure water purification system	Millipore, USA
Glasswares	

### 3.1.6 Electrochemical measurements of AA, DA and UA

Table 3.5 shows the instruments and apparatus for the electrochemical measurements of AA, DA and UA.

**Table 3.5** Instruments and apparatus for the electrochemical measurements of AA, DA and UA

Instruments and apparatus	Suppliers
AutoLab PG 30 potentiostat/galvanostat	Metrohm, The Netherlands
Milli-Q ultrapure water purification system	Millipore, USA
Micropipette and tips	Eppendorf, Germany
Vortex mixer	LMS, Japan
Faraday cage	
Glasswares	

## 3.2 Chemicals

### 3.2.1 GQDs synthesis

The chemicals for the GQDs synthesis are listed in Table 3.6.

**Table 3.6** Information of the chemicals for the GQDs synthesis

Chemicals	Suppliers
Citric acid monohydrate (AR grade)	Carlo Erba, USA
Sodium hydroxide (AR grade)	Sigma-Aldrich, Germany
Milli-Q ultrapure water ( $R \geq 18.2 \text{ M}\Omega \cdot \text{cm}$ )	Milli-Q ultrapure water purification system, Millipore, USA

### 3.2.2 Fabrication of the GQDs/IL-SPCE

The chemicals for the fabrication of the GQDs/IL-SPCE are shown in Table 3.7.

**Table 3.7** List of the chemicals for the fabrication of the GQDs/IL-SPCE

Chemicals	Suppliers
1-butyl-3-methylimidazolium hexafluorophosphate (AR grade)	Sigma-Aldrich, Germany
Carbon ink	Gwent, UK
Silver/silver chloride paste	Gwent, UK

### 3.2.3 Electrochemical measurements of AA, DA and UA

The chemicals for the electrochemical measurements of AA, DA and UA are described in Table 3.8.

**Table 3.8** List of the chemicals used for the electrochemical measurements of AA, DA and UA

Chemicals	Suppliers
L-ascorbic acid (AR grade)	Merck, Germany
Dopamine hydrochloride (AR grade)	Sigma-Aldrich, Germany
Uric acid (AR grade)	Wako, Japan
Milli-Q ultrapure water ( $R \geq 18.2 \text{ M}\Omega \cdot \text{cm}$ )	Milli-Q ultrapure water purification system, Millipore, USA
Potassium phosphate monobasic (AR grade)	Sigma-Aldrich, Germany
Potassium phosphate dibasic (AR grade)	Sigma-Aldrich, Germany

### 3.2.4 Sample preparations

The chemicals used in the sample preparations are listed in Table 3.9.

**Table 3.9** List of the chemicals in the sample preparations

Chemicals	Suppliers
L-ascorbic acid (AR grade)	Merck, Germany
Dopamine hydrochloride (AR grade)	Sigma-Aldrich, Germany
Uric acid (AR grade)	Wako, Japan
Milli-Q ultrapure water ( $R \geq 18.2 \text{ M}\Omega \cdot \text{cm}$ )	Milli-Q ultrapure water purification system, Millipore, USA
Potassium phosphate monobasic	Sigma-Aldrich, Germany
Potassium phosphate dibasic	Sigma-Aldrich, Germany



### 3.3 Chemical preparations

#### 3.3.1 Preparation of solution for GQDs synthesis

##### 3.3.1.1 10 mg/mL of sodium hydroxide solution

A 10 mg/mL of sodium hydroxide solution was prepared by dissolving 1 g of sodium hydroxide in 100 mL of Milli-Q water.

##### 3.3.1.2 1 mg/mL of citric acid solution

For preparation of 1 mg/mL of citric acid solution, 0.1 g of citric acid was dissolved in 100 mL of Milli-Q water.

#### 3.3.2 Preparation of solutions for the determination of AA, DA and UA

##### 3.3.2.1 0.1 M potassium phosphate monobasic solution

A 0.1 M potassium phosphate monobasic solution was prepared by dissolving 4.35 g of potassium phosphate monobasic in 250 mL of Milli-Q water.

##### 3.3.2.2 0.1 M potassium phosphate dibasic solution

A 0.1 M potassium phosphate dibasic solution was obtained by dissolving 3.40 of potassium phosphate monobasic in 250 mL of Milli-Q water.

##### 3.3.2.3 0.1 M phosphate buffer solution (PBS)

A 0.1 M PBS with various pH values was prepared by mixing stock solution of 0.1 M potassium phosphate monobasic solution and 0.1 M potassium phosphate dibasic solution as shown in table 3.10. Then, the pH of mixing solution was adjusted by adding sodium hydroxide or hydrochloric acid.

**Table 3.10** Preparation of 0.1 M PBS at various pH with the final volume of 100 mL

pH	Volume of 0.1 M potassium phosphate monobasic solution (mL)	Volume of 0.1 M potassium phosphate dibasic solution (mL)
5.0	0.8	99.2
6.0	11.1	88.9
7.0	58.7	41.3
8.0	96.3	3.7

#### 3.3.2.4 10 mM AA solution

A 10 mM stock solution of AA was prepared by dissolving 0.040x mg of L-ascorbic acid in 25 mL of 0.1 M PBS pH 4.0.

#### 3.3.2.5 1 mM DA solution

A 1 mM stock solution of DA was prepared by dissolving 0.004x mg of dopamine hydrochloride in 25 mL of 0.1 M PBS pH 4.0.

#### 3.3.2.6 1 mM UA solution

First, 0.004x mg of UA was dissolved in 0.1 M sodium hydroxide. After that, the mixture was adjusted to 25 mL with 0.1 M PBS pH 4.0.

### 3.4 Synthesis of GQDs

The GQDs was synthesized by directly pyrolyzing citric acid according to the previously described procedure [27, 35]. 2 g of citric acid was heated to 200 °C for 5 min to obtain citric acid in liquid form. Then, the color of liquid changed from colorless to orange in 30 min. After that, the aliquot of orange liquid was added into 100 mL of 10 mg/mL of sodium hydroxide solution with continuous vigorous stirring.

Then, the aqueous solution of GQDs was adjusted to pH 8.0 with 1 mg/mL of citric acid solution. The final solution was stored in a refrigerator at 4 °C.

### 3.5 Characterization of GQDs

A photograph of GQDs solution was acquired by a smart phone camera. The UV-Vis spectrum of GQDs was obtained by the UV-Vis spectrophotometer using a 1.0 cm quartz cell. Fluorescence spectrum was recorded using a Cary Eclipse fluorescence spectrophotometer with the excitation wavelength of 365 nm. The morphology and particles size of GQDs were analyzed using transmission electron microscope. The sample for transmission electron microscopic measurement was prepared by drop casting of GQDs solution onto a copper grid and allowed to dry at room temperature.

### 3.6 Fabrication of the electrochemical sensors

The modified screen printed carbon electrode was fabricated in-house via screen-printing method. The mesh for printing of the electrodes consisting of reference electrode, working electrode, counter electrode and connector position was defined the geometry and size as shown in Figure 3.1 and 3.2. The preparation of modified screen-printed carbon electrode was presented as follows. First, the polyvinyl chloride (PVC) substrate was cut to obtain a size 12 x 14 cm. Second, the silver ink was printed onto PVC substrate through the mesh to form the reference electrode and dried at 55 °C for 1 h. Third, the mixture of 1.0 g carbon ink and 0.01 g 1-butyl-3-methylimidazolium hexafluorophosphate ([BMIM]PF<sub>6</sub>) IL was printed onto PVC to form working electrode, counter electrode and connector positions, and then dried in an oven at 55 °C for 1 h. Finally, 7.5 µL of GQDs was dropped onto the surface of working electrode and dried at room temperature. The obtained in-house screen-printed carbon electrode consisted of modified working electrode, reference silver/silver chloride electrode and counter carbon electrode as shown in Figure 3.3

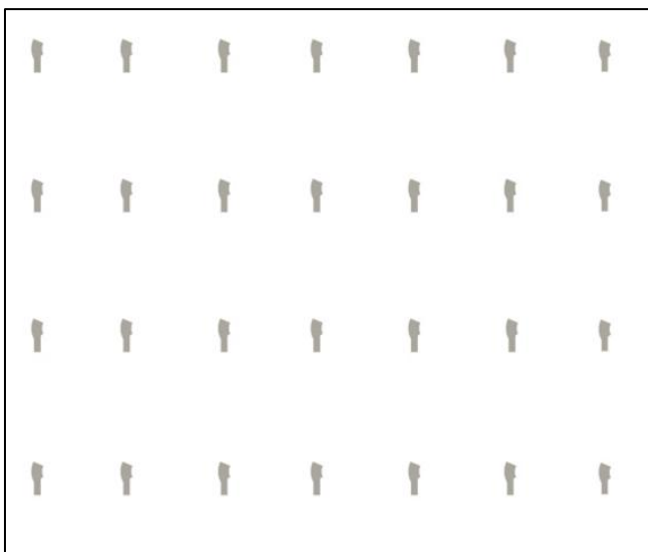


Figure 3.1 Pattern of reference electrode

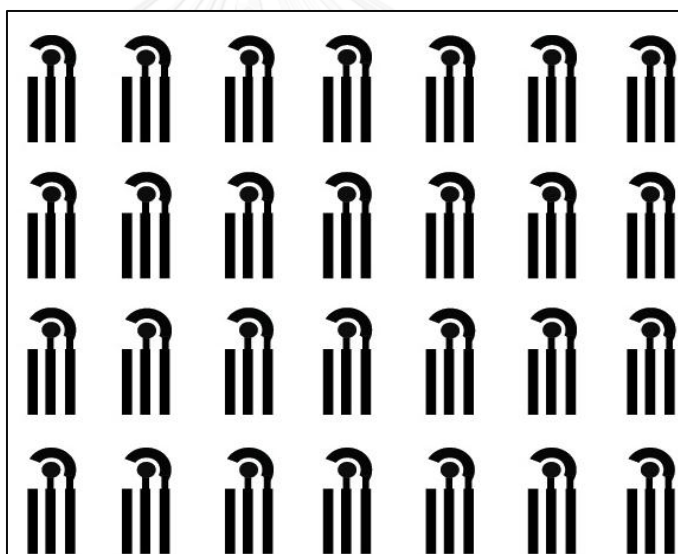
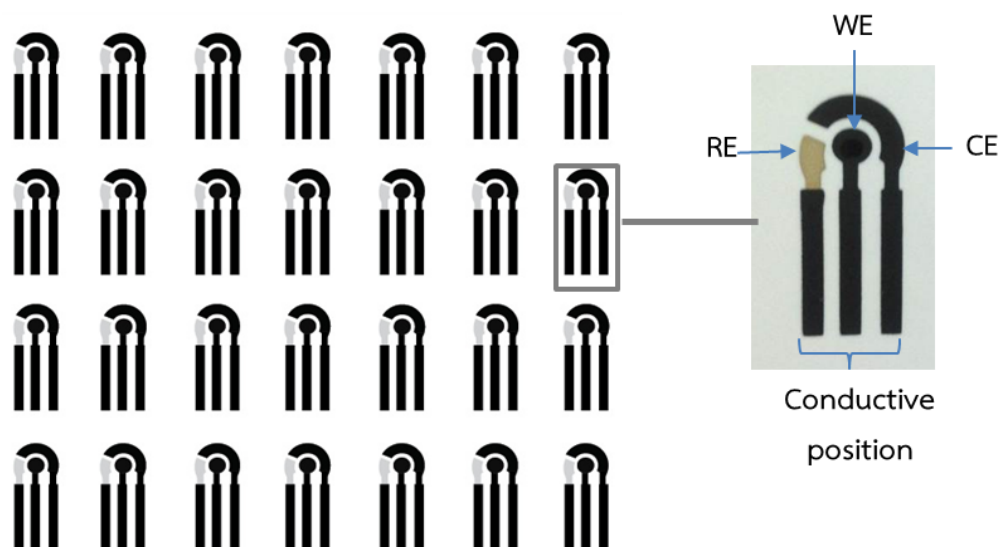


Figure 3.2 Template of working electrode, counter electrode and connector position



**Figure 3.3** The In-house screen-printed carbon electrode with three integrated electrodes (WE: working electrode, RE: reference electrode and CE: counter electrode)

### 3.7 Electrochemical experiments

Electrochemical experiments were carried out using an all-in-one modified screen-printed carbon electrode consisting of (i) GQDs and IL modified working electrode with projective surface of area =  $12.56 \text{ mm}^2$ , (ii) silver/silver chloride as pseudo-reference electrode and (iii) carbon as the counter electrode. Electrochemical procedure was performed by dropping a  $60 \mu\text{L}$  of testing solution onto the surface area of electrochemical sensor via micropipette, and electrochemical experiment was conducted using an AutoLab PG 30 potentiostat/galvanostat controlled by NOVA 1.10 software. The electrode pre-treatment was performed by applying conditioning potential of  $+1.70 \text{ V}$  vs.  $\text{Ag}/\text{AgCl}$  for  $90 \text{ s}$  in  $0.1 \text{ M}$  PBS pH  $7.0$ . After that,  $60 \mu\text{L}$  drop of  $0.1 \text{ M}$  PBS pH  $4.0$  as electrolyte solution was added onto a pre-treated modified screen-printed carbon electrode and then the background current was recorded. Finally,  $60 \mu\text{L}$  of AA, DA and UA in electrolyte solution was placed onto the surface of electrode and CV or DPV was performed. All experiments were carried out at room temperature using a new electrode for each assay.

### 3.8 Electrode characterization

Characterization of the bare SPCE, IL-SPCE and GQDs/IL-SPCE was compared by CV, DPV and SEM. For electrochemical characterization, CV was performed in the presence of individual AA, DA and UA dissolved in 0.1 M PBS pH 4.0. The CV responses were recorded in the potential range of -1.0 to +1.0 V with the scan rate of 50 mV/s. Moreover, the electrochemical activity of the mixture of AA, DA and UA at different electrodes was investigated and compared using DPV. The surface morphology was accomplished by SEM.

### 3.9 Optimization of modified electrode

#### 3.9.1 The amount of IL

The effect of the amount of IL on electrochemical oxidation responses of AA, DA and UA at GQDs/IL-SPCE was studied. Various amounts of IL, 0, 5, 10, 15, 20, 25 and 30 mg, were mixed into 1 g of carbon ink and screen-printed to form working electrode using the same protocol as described previously.

#### 3.9.2 The volume of GQDs

The influence of the volume of GQDs on the DPV responses of AA, DA and UA was investigated by variation of the GQDs solution volume at 0, 2.5, 5.0, 7.5 and 10.0  $\mu\text{L}$ .

#### 3.9.3 The effect of electrode pretreatment condition

##### 3.9.3.1 Pretreatment potential

Electrochemical pretreatment of GQDs/IL-SPCE was performed by anodic oxidation in 0.1 M PBS (pH 7.0). The effect of pretreatment potential on the current responses of AA, DA and UA at GQDs/IL-SPCE was examined by variation of pretreatment potential at +1.5, +1.6, +1.7, +1.8, +1.9 and +2.0 V.

### 3.9.3.2 Pretreatment time

In order to study the effect of pretreatment time at GQDs/IL-SPCE, variation of pretreatment time at 0, 30, 60, 90 and 120 s was examined.

### 3.9.4 The effect of scan rate

The effect of scan rate on peak currents of AA, DA and UA at GQDs/IL-SPCE was explored in the range of 10 - 70 mV.

### 3.9.5 The influence of pH on the anodic peak currents of AA, DA and UA

The influence of pH on the oxidation of AA, DA and UA at GQDs/IL-SPCE was studied in the range of pH 2 to 9.

### 3.10 Optimization of the DPV parameter

Various DPV parameters were optimized to provide the best electrochemical response for the simultaneous determination of three analytes of interest. Table 3.11 shows the examined DPV parameters which generally affected on height, shape and separation of these peak responses.

**Table 3.11** The optimized parameters for DPV measurement using GQDs/IL-SPCE.

DPV parameters	Examined values
Step potential	1.0 to 3.0 mV
Pulse amplitude	20 to 70 mV
Pulse width	0.2 to 0.6 s
Pulse time	0.01 to 0.05 s

### 3.11 Analytical performance

#### 3.11.1 Linearity, LOD and LOQ

Two types of linear calibration curve for the simultaneous DPV detection of AA, DA and UA using GQDs/IL-SPCE under optimized conditions were investigated.

- (i) The concentration of one analyte was varied, whereas those of the other two compounds were kept constant.
- (ii) The concentrations of three analytes were simultaneously altered.

The average oxidation peak current for triplicate measurements was used to plot the calibration curve which the linear range of the simultaneous of AA, DA and UA was obtained. The limit of detection (LOD) and the limit of quantification (LOQ) were determined statistically from the calibration curve of AA, DA and UA, which were calculated from  $3S_b/S$  and  $10S_b/S$ .  $S_b$  is the standard deviation from seven replicate of blank measurements ( $n=7$ ) and  $S$  is the slope of the calibration curve.

#### 3.11.2 Reproducibility

The reproducibility of GQDs/IL-SPCE was investigated by the simultaneous determination of a mixture solution containing 300  $\mu\text{M}$  of AA, 5  $\mu\text{M}$  of DA and 5  $\mu\text{M}$  of UA by DPV at five different sensors. The reproducibility was evaluated in the term of relative standard deviation (RSD), using the following formula:

$$\%RSD = \frac{\text{Standard deviation}}{\text{Mean}} \times 100$$



### 3.11.3 Interference study

Several compounds of common co-existing in biological sample were selected to assess the anti-interference ability of GQDs/IL-SPCE. The influence of potentially interfering substance on the selectivity of system was studied by testing mixture solution of 300  $\mu\text{M}$  of AA, 5  $\mu\text{M}$  of DA and 5  $\mu\text{M}$  of UA in the presence of foreign compounds including citric acid, glucose, L-cysteine, NaCl, KCl,  $\text{MgSO}_4$ ,  $\text{CaCl}_2$  and  $\text{Zn}(\text{NO}_3)_2$  at 1000  $\mu\text{M}$ .

## 3.12 Real sample analysis

### 3.12.1 Determination of AA in Vitamin C tablets

Tablet of vitamin C (labeled 500 mg vitamin C per tablet) was completely ground and dissolved in 50 mL of Milli-Q water and filtered through a whatman filter paper No. 1 to remove the particle matter. The resulting solution was diluted 100 times with 0.1 M PSB (pH 4.0) and measured by DPV using optimal conditions. The standard addition method was used to determine AA in vitamin C tablet.

### 3.12.2 Determination of DA in DA injection

DA injection solution (250 mg/10 mL) was analyzed directly after it was diluted with 0.1 M PBS (pH 4.0) using the standard addition method.

### 3.12.3 Determination of AA, DA and UA in human serum

For the simultaneous determination of AA, DA and UA in human serum sample, lyophilized human control serum sample (level I) was purchased from Nissui Pharmaceutical (Tokyo, Japan). The sample was diluted with 0.1 M PBS (pH 4.0) and used for the detection without any further pretreatment. Then, the

standard addition method was applied to simultaneously determine AA, DA and UA. The recovery of the spike was calculated as follows:

$$\% \text{Recovery} = \frac{C_s}{C_u} \times 100$$

Where  $C_s$  is the concentration of analyte found in spiked sample and  $C_u$  is the concentration of analyte that added into the sample.



## CHAPTER IV

### RESULTS AND DISCUSSION

This chapter presents results and discussion consisting of 5 topics which are GQDs synthesis, the electrochemical responses of AA, DA, and UA at the modified electrode, the optimization of the modified electrode and experimental conditions, analytical performance and analytical application to real samples.

#### 4.1 Characterizations of synthesized GQDs

##### 4.1.1 UV-Vis and fluorescence spectroscopy

GQDs nanomaterial was synthesized by carbonization of citric acid according to a reported literature procedure [27, 35]. The aqueous solution of GQDs exhibited a blue color under excitation at 365 nm by black light as shown in the inset of Figure 4.1. In addition, Figure 4.1 displays two spectra obtained from UV-Vis absorption and fluorescence spectroscopy (FL).

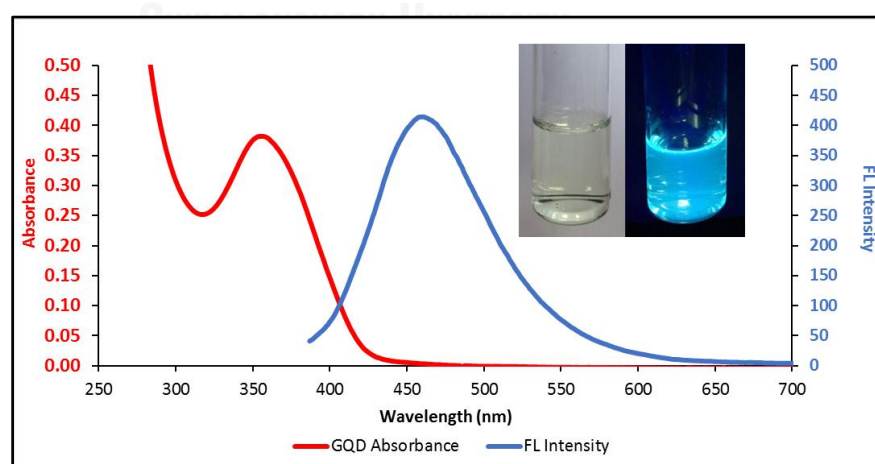


**Figure 4.1** UV-Vis absorption (red line) and FL spectra (blue line) of the synthesized GQDs. Inset: photographs of the GQDs solution taken under visible light (left) and under black light (right).

For the absorption spectra of GQDs (red line), the absorption peak at 365 nm was assigned to the  $n - \pi^*$  transition of C=O, and the strong background absorption below 300 nm was assigned to the  $\pi - \pi^*$  transition of C=C. The fluorescence behavior of GQDs (blue line), the maximum emission at about 460 nm was obtained with an excitation wavelength of 365 nm, corresponding to the excitation spectra [36].

#### 4.1.2 Transmission electron microscopy

The morphology and particle size of GQDs was studied by transmission electron microscopy (TEM). TEM image in Figure 4.2 clearly indicates that the prepared GQDs are spherical shape and well monodisperse nanoparticles. The diameters of GQDs were mainly distributed in the range of 2.5-12.5 nm with average diameter of 5.5 nm. These results were high agreement with those from previous published report [27].

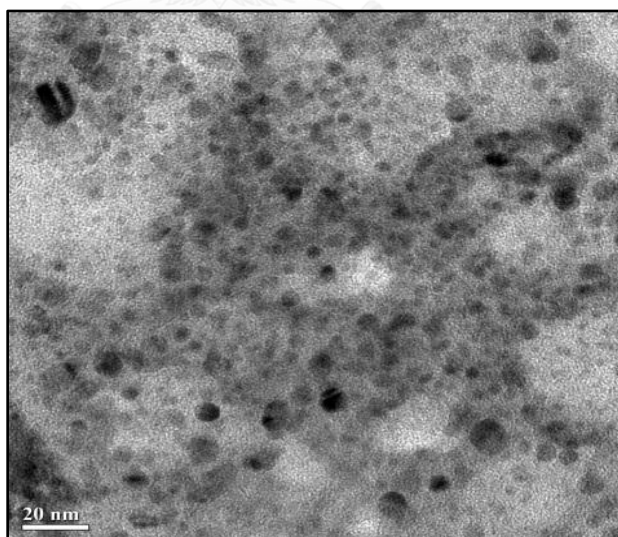


**Figure 4.2** TEM image of the synthesized GQDs.

## 4.2 Electrochemical characterization of GQDs/IL-SPCE

The electrochemical behavior of mixture of AA, DA, and UA at the bare-SPCE, IL-SPCE, GQDs/SPCE and GQDs/IL-SPCE was examined by DPV. As shown in Figure 4.3, the anodic peak responses obtained from bare electrode is indistinguishable, indicating the poor selectivity and sensitivity. For the IL-SPCE, three well-defined oxidation peaks were separated and observed at potentials of 0.02, 0.16, and 0.32 V vs. Ag/AgCl corresponding to the oxidation of AA, DA, and UA, respectively. At GQDs/SPCE, three separable peaks appeared at -0.03, 0.15, and 0.29 V vs. Ag/AgCl. Moreover, the current signal of dopamine is greatly enhanced. In the case of our proposed GQDs/IL-SPCE, the three electroactive species AA, DA, and UA were oxidized with well-defined and distinguishable sharp peaks at potentials of -0.03, 0.18, and 0.34 V vs. Ag/AgCl, respectively, with higher anodic peak currents than the bare electrode. The large separation of oxidation peak potentials of AA-DA, DA-UA and AA-UA were found to be 198, 163, and 361 mV, respectively.

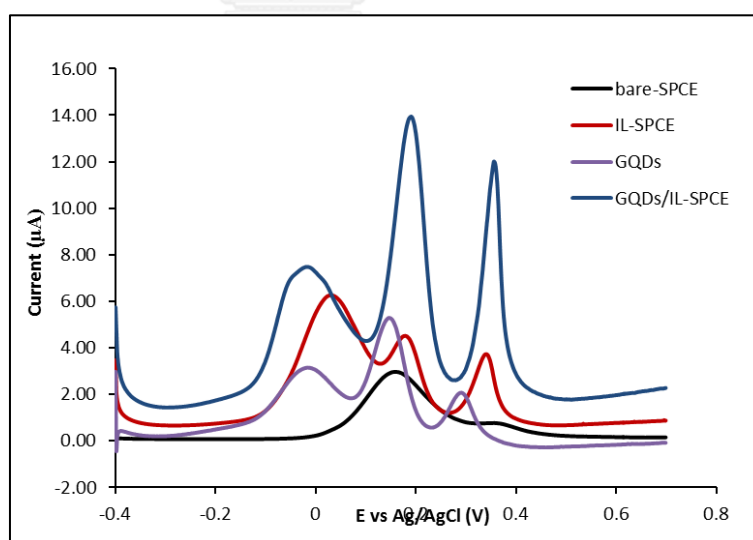


**Figure 4.3** DPV at bare-SPCE, IL-SPCE, GQDs/SPCE and GQDs/IL-SPCE of ternary mixture of 400  $\mu\text{M}$  AA, 10  $\mu\text{M}$  DA and 10  $\mu\text{M}$  UA in 0.1 M PBS (pH 4.0).

These results suggest that the GQDs/ILs-SPCE combines the excellent electrochemical properties of IL and GQDs. The performance of electrochemical activity of AA, DA and UA was enhanced from the high ionic conductivity of IL [37]. The  $\pi$ - $\pi$  interaction between phenyl structure of DA and hexagonal carbon structure of GQDs, increased sensitivity of analyte because it could induce analytes to the electrode surface. Besides, functional group of GQDs can form different types of hydrogen bonding with AA and UA, which improve sensitivity of electrode as well [32, 38, 39]. This indicates that the GQDs/IL-SPCE can be used effectively for the simultaneous determination of AA, DA, and UA in their mixture. Therefore, GQDs and IL were selected as an appropriate electrode modifier for further experiments.

#### 4.3 Morphological characterization of the GQDs/IL-SPCE

The surface morphology of the bare-SPCE, IL-SPCE, and GQDs/IL-SPCE was investigated by scanning electron microscopy (SEM). As shown in Figure 4.4, the surface of bare-SPCE was occupied by the disordered distribution of graphite flakes. For IL-SPCE (Figure 4.5), a relatively compact and homogeneous surface was observed, indicating the good adherence of IL with graphite particles. Therefore, the IL and carbon ink would firmly bind together to form a stable solid composition [40]. When GQDs were deposited onto IL-SPCE (Figure 4.6), the surface of the modified electrode changed to a smooth and uniform layered GQDs film, presented the forming of GQDs on the electrode surface.

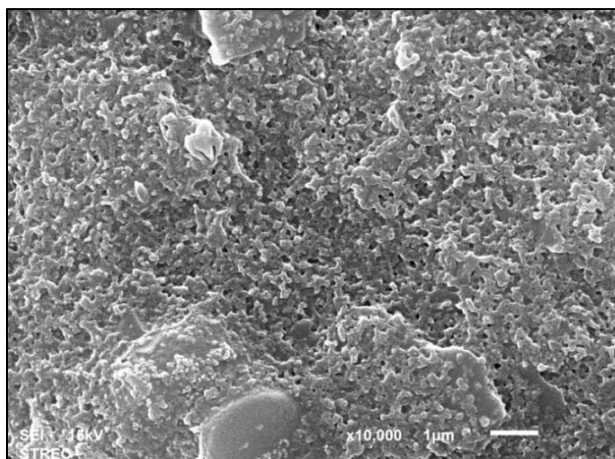


Figure 4.4 SEM image of bare-SPCE.

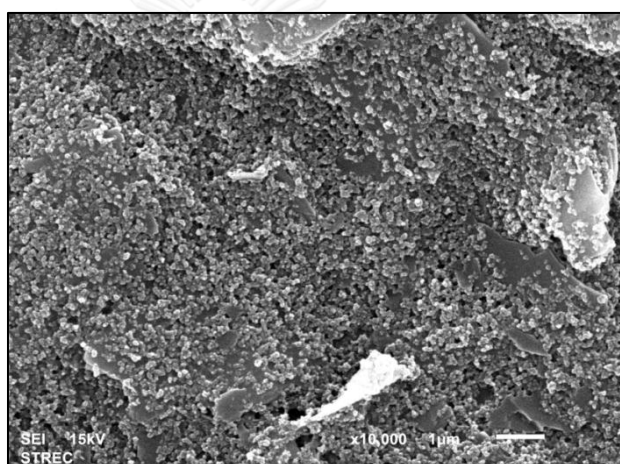


Figure 4.5 SEM image of IL-SPCE.

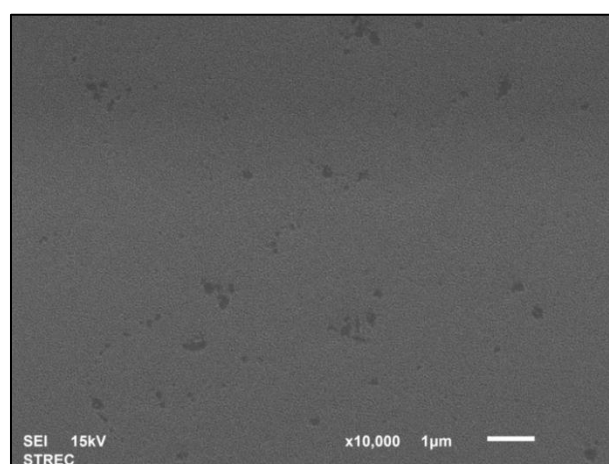
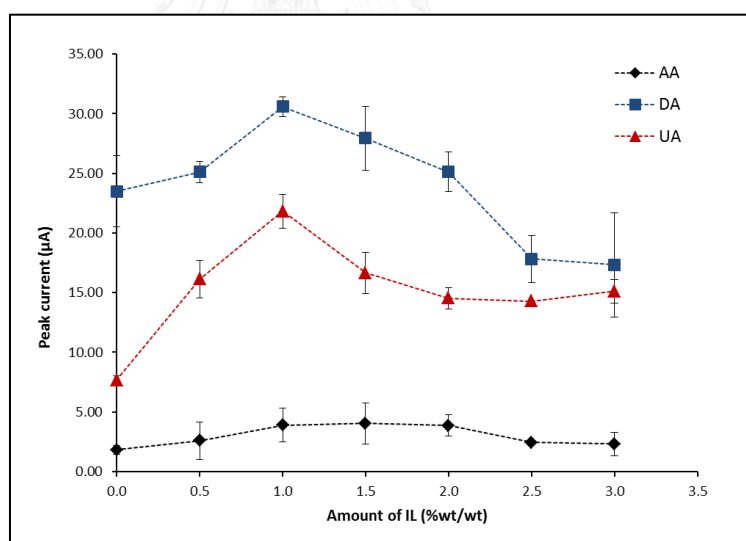


Figure 4.6 SEM image of GQDs/IL-SPCE.

## 4.4 Optimization of modified electrode

### 4.4.1 The amount of IL

IL was used as electrode modifier by mixing into the carbon ink before screen printing onto PVC to form the working electrode. The effect of the amount of IL on the electrochemical responses of AA, DA, and UA was studied in the range of 0 - 3 % wt/wt. As shown in Figure 4.7, the anodic peak currents of AA, DA, and UA gradually increased with increasing IL content and reached to a maximum point at IL content of 1% wt/wt. When IL content was higher than 1% wt/wt these peak currents apparently decreased. This is because the excess IL amount significantly increased capacitance (or background current) of the modified electrode [29, 41]. Therefore, the optimal amount of IL was 1 %wt/wt and following experiments were carried out at this amount.



**Figure 4.7** Effect of the IL amount on the peak currents of 1 mM AA, 1 mM DA, and 1 mM UA in 0.1 M PBS (pH 7.0) at GQDs/IL-SPCE. Data are shown as the mean  $\pm$  SD and are derived from three replicates.



#### 4.4.2 The volume of GQDs

GQDs was modified onto the surface of working electrode via drop casting the GQDs solution. The effect of the volume of GQDs solution on the DPV responses of 1 mM AA, DA, and UA in 0.1 M PBS (pH 7.0) was examined in the range of 0.0 – 10.0  $\mu\text{L}$  (Figure 4.8). The anodic peak currents of AA at various amounts of GQDs were not significantly difference, whereas the anodic peak currents of DA and UA increased as the amount of GQDs increased from 0.0 to 7.5  $\mu\text{L}$  then decreased at higher amount of GQDs. This can be explained that high amount of GQDs leads to the aggregation of GQDs, resulting in the decreased electrochemical performance of the modified electrode towards the detection of AA, DA and UA. Hence, a 7.5  $\mu\text{L}$  was selected as an optimal GQDs solution volume.

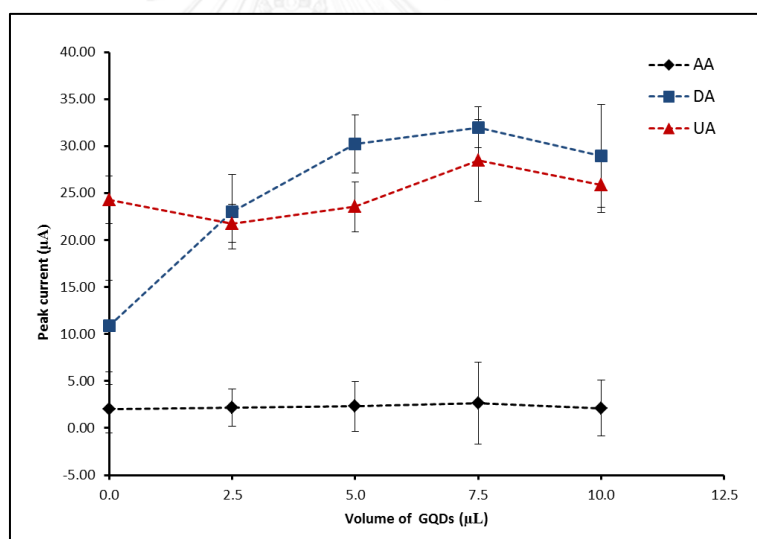


**Figure 4.8** Effect of the amount of GQDs solution on the peak currents of 1 mM AA, 1 mM DA and 1 mM UA in 0.1 M PBS (pH 7.0) at GQDs/IL-SPCE. Data are shown as the mean  $\pm$  SD and are derived from three replicates.

### 4.4.3 The effect of electrode pretreatment condition

#### 4.4.3.1 Pretreatment potential

Electrode pretreatment is usually required to activate the surface of GQDs [28, 42]. The effect of pretreatment potential of GQDs/IL-SPCE was investigated at different potentials ranging between -0.5 to +2.0 V vs. Ag/AgCl for 3 min. The results in Figure 4.9 show that, when the pretreatment potential was increased, the anodic peak currents of three analytes also increased, and then their current decreased at more positive potentials. Although the peak currents obtained from pretreatment potential at 1.8 V vs. Ag/AgCl was the highest, the background current was higher than at 1.7 V (see Figure 4.10). As a result, the pretreatment potential at 1.7 V was chosen for this work, which are consistent with previously reported [42].

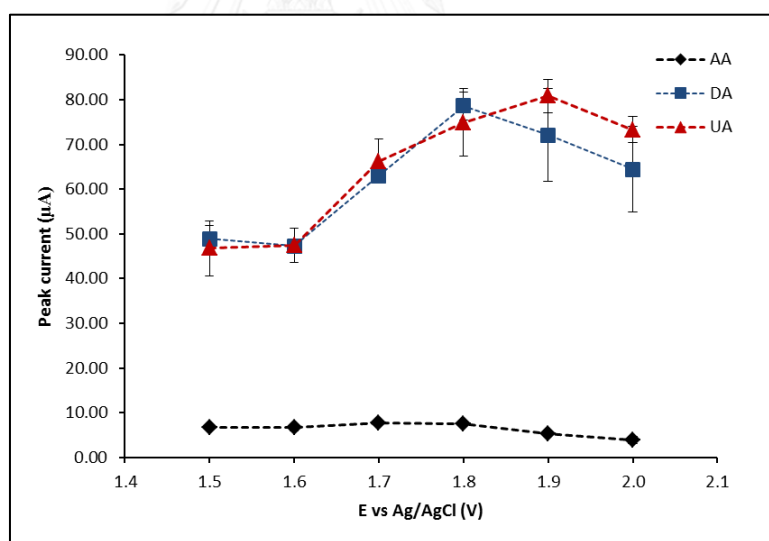


**Figure 4.9** Effect of the pretreatment potential on the peak currents of 1 mM AA, 1 mM DA and 1 mM UA in 0.1 M PBS (pH 7.0) at GQDs/IL-SPCE. Data are shown as the mean  $\pm$  SD and are derived from three replicates.

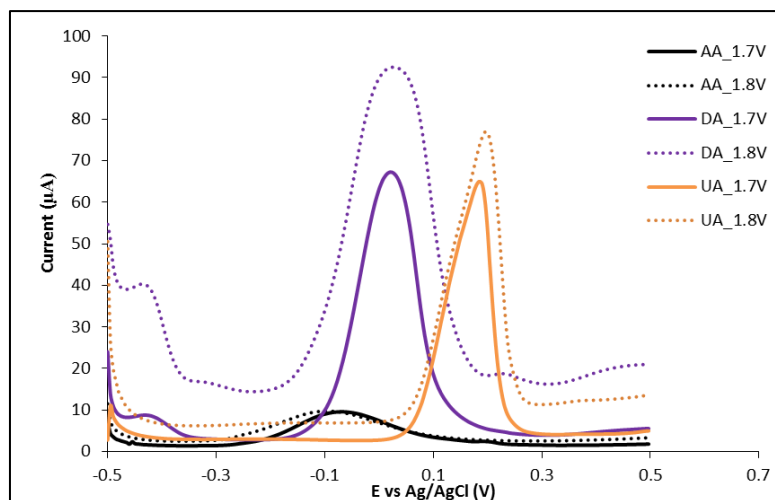


**Figure 4.10** Effect of pretreatment potential at 1.7 V and 1.8 V on the DPV responses of 1 mM AA, 1 mM DA and 1 mM UA in 0.1 M PBS (pH 7.0) at GQDs/IL-SPCE.

#### 4.4.3.2 Pretreatment time

The effect of pretreatment time of the GQDs/IL-SPCE was studied using pretreatment potential at 1.70 V vs. Ag/AgCl for different times (0, 30, 60, 90, and 120 s). The results are shown in Figure 4.11. At the pretreatment time of 90 s, the peak current of DA was highest, the peak current of AA remained constant and the peak current of UA was still performed good sensitivity. Thus, the pretreatment time of 90 s was selected for further study. These optimal pretreatment conditions (e.g. potential and time) are essential for the preparation of modified electrode prior to electrochemical measurement.

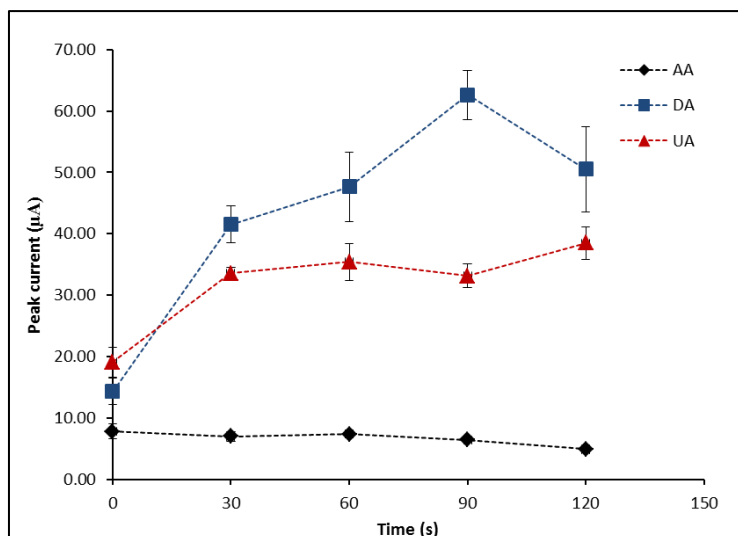


**Figure 4.11** Effect of the pretreatment time on the peak currents of 1 mM AA, 1 mM DA and 1 mM UA in 0.1 M PBS (pH 7.0) at GQDs/IL-SPCE. Data are shown as the mean  $\pm$  SD and are derived from three replicates.

#### 4.4.4 Effect of scan rate

To investigate the kinetic electrode reactions, Figure 4.12, 4.13 and 4.14 display the cyclic voltammograms of 1 mM AA, 1 mM DA, and 1 mM UA, respectively, in 0.1 M PBS (pH 4.0) with different scan rates (10-70 mV/s) at the GQDs/IL-SPCE. The results (Figure 4.15-4.17) show that the oxidation peak currents of AA, DA and UA were linearly proportional to the square root of scan rate via the linear equation of  $i_{p,AA}(\mu A) = 1.7814v^{1/2} \text{ (mV/s)} - 0.2702$  ( $R^2 = 0.9921$ ),  $i_{p,DA}(\mu A) = 3.8934v^{1/2} \text{ (mV/s)} - 1.4229$  ( $R^2 = 0.9971$ ), and  $i_{p,UA}(\mu A) = 3.3935v^{1/2} \text{ (mV/s)} + 1.9151$  ( $R^2 = 0.9935$ ), where  $i_p$  is peak current and  $v$  is scan rate. The above results demonstrate that the oxidation reaction of AA, DA, and UA on the GQDs/IL-SPCE are diffusion-controlled process.

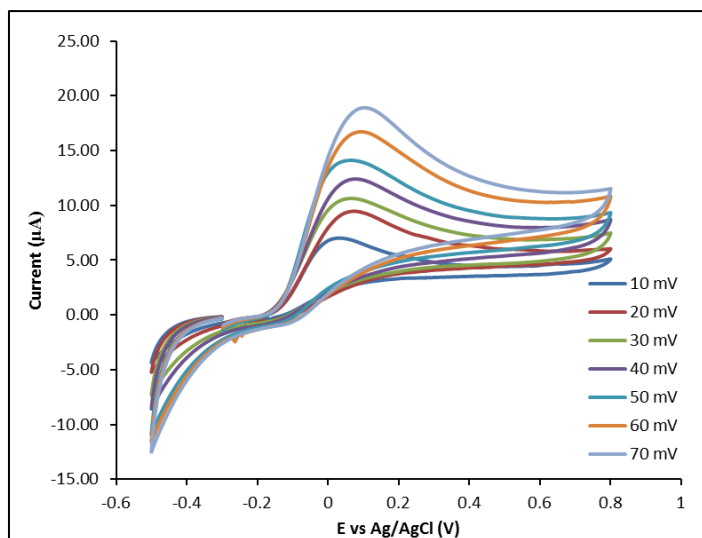


**Figure 4.12** Cyclic voltammograms of 1 mM AA in 0.1 M PBS (pH 4.0) on GQDs/IL-SPCE at different scan rates of 10, 20, 30, 40, 50, 60, and 70 mV/s.

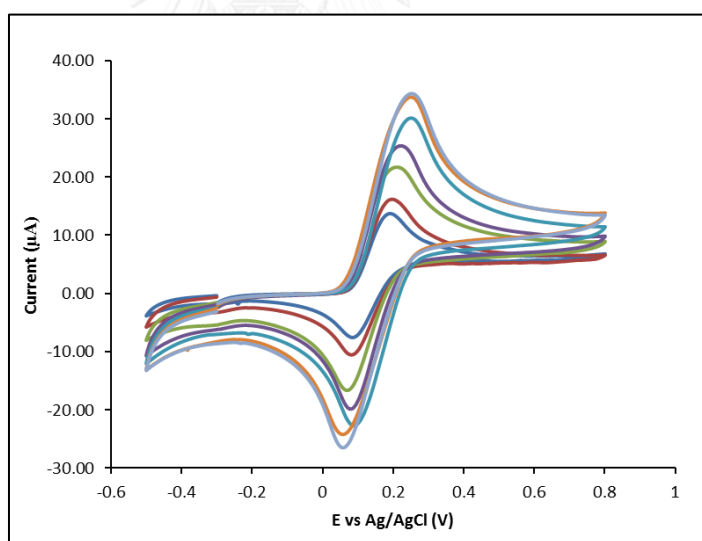


**Figure 4.13** Cyclic voltammograms of 1 mM DA in 0.1 M PBS (pH 4.0) on GQDs/IL-SPCE at different scan rates of 10, 20, 30, 40, 50, 60, and 70 mV/s.

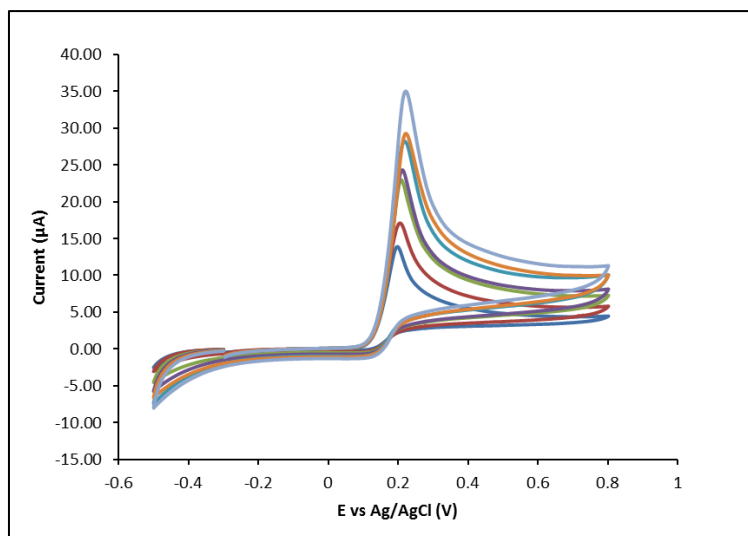


**Figure 4.14** Cyclic voltammograms of 1 mM UA in 0.1 M PBS (pH 4.0) on GQDs/IL-SPCE at different scan rates of 10, 20, 30, 40, 50, 60, and 70 mV/s.

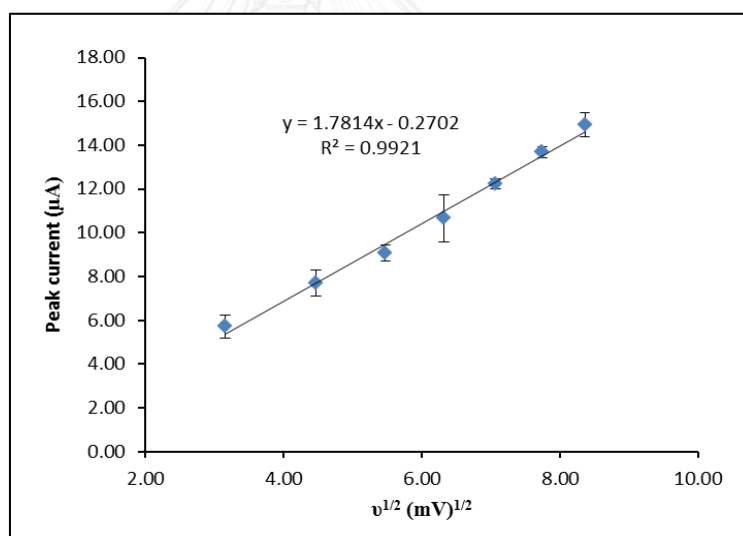


**Figure 4.15** Plots of anodic peak currents of AA vs. square root of scan rates. Data are shown as the mean ± SD and are derived from three replicates.

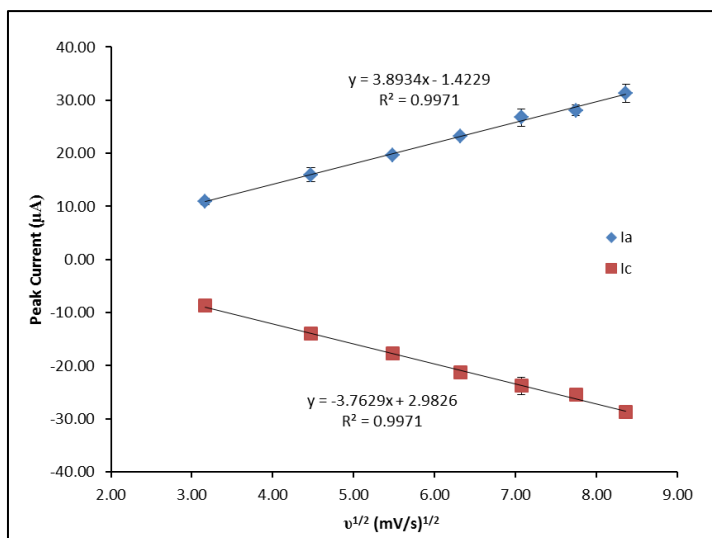


**Figure 4.16** Plots of anodic and cathodic peak currents of DA vs. square root of scan rates. Data are shown as the mean  $\pm$  SD and are derived from three replicates.

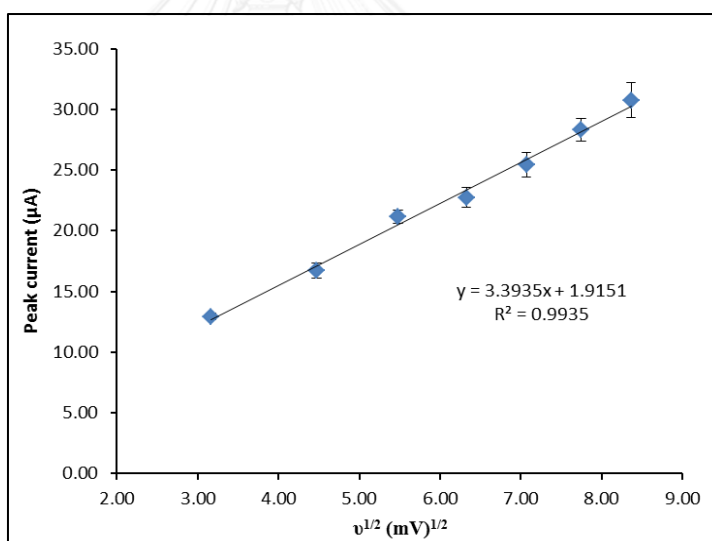


**Figure 4.17** Plots of anodic peak currents of UA vs. square root of scan rates. Data are shown as the mean  $\pm$  SD and are derived from three replicates.

#### 4.4.5 The influence of pH on the anodic peak currents of AA, DA and UA

The influence of pH on the peak currents and peak potentials of the simultaneous detection of AA, DA, and UA in the range from pH 2.0 to 9.0 was investigated by DPV. As shown in Figure 4.18, the oxidation peak potentials ( $E_{pa}$ ) of these three biomolecules shifted negatively with the higher pH values, indicating that the electrocatalytic oxidation of these analytes at the modified electrode is a pH-dependent reaction. The relationship between peak potential and the pH value was obtained as follows:

$$E_{pa,AA} \text{ (V)} = 0.2139 - 0.0460\text{pH} \text{ (R}^2=0.946)$$

$$E_{pa,DA} \text{ (V)} = 0.4498 - 0.0558\text{pH} \text{ (R}^2=0.968),$$

$$E_{pa,UA} \text{ (V)} = 0.6283 - 0.0617\text{pH} \text{ (R}^2=0.970)$$

The slopes were found to be -46, -55.8, and -61.7 mV/pH, which are close to the theoretical value of -59 mV/pH indicating that the electrode process is two-proton and two-electron transfer process [43].

In addition, the pH value of the supporting electrolyte also affects the current response of three analytes. Figure 4.19 illustrated peak current of AA, DA and UA was dependent on the pH. The 0.1 M PBS (pH 4.0) can be used in order to compromise for the sensitivity of all analytes of interest. Therefore, pH of PBS at 4.0 was selected as an optimal parameter for the further experiment.



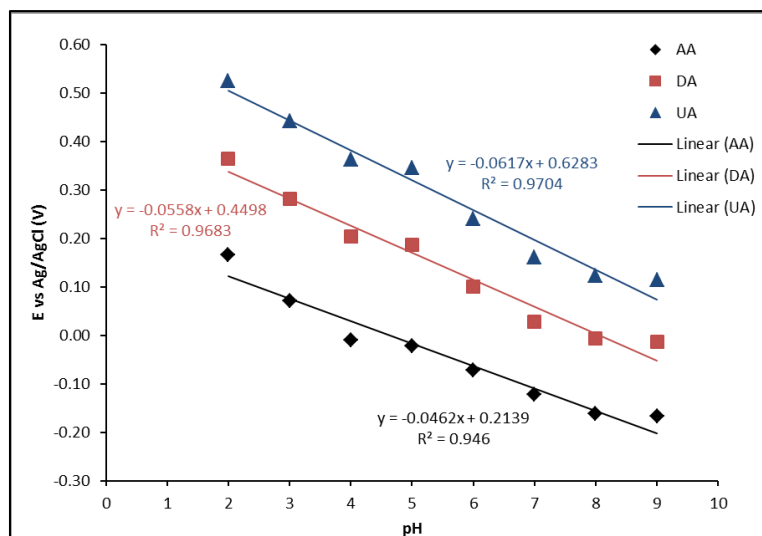


**Figure 4.18** Effect of pH on the DPV peak potentials of 1 mM AA, 5  $\mu$ M DA and 10  $\mu$ M UA in 0.1 M PBS at GQDs/IL-SPCE. Data are shown as the mean  $\pm$  SD and are derived from three replicates.

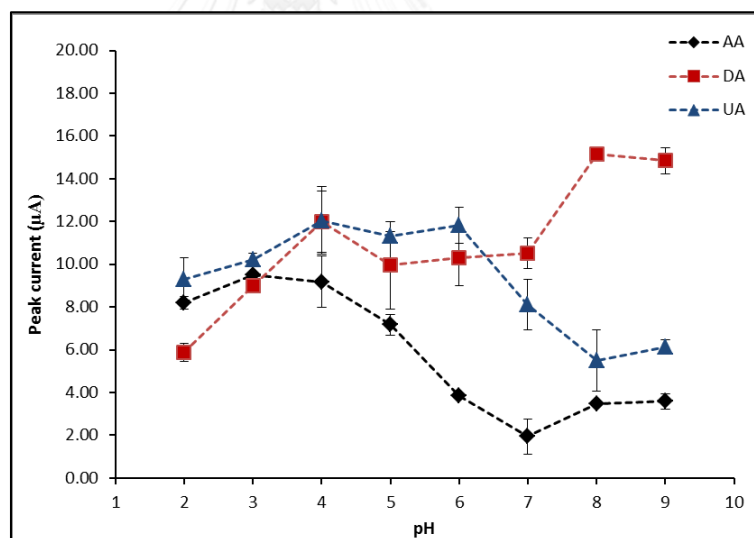


**Figure 4.19** Effect of pH on the DPV peak currents of 1 mM AA, 5  $\mu$ M DA and 10  $\mu$ M UA in 0.1 M PBS at GQDs/IL-SPCE. Data are shown as the mean  $\pm$  SD and are derived from three replicates.

#### 4.5 Optimization of the differential pulse voltammetric conditions

The simultaneous detection of AA, DA, and UA by DPV at GQDs/IL-SPCE was optimized to obtain best electrochemical responses. The DPV conditions including step potential, pulse amplitude, pulse width and pulse time were most influence on the height, shape and separation of these peak responses. Begin with step potential, the effect of this parameter on the anodic peak currents of AA, DA and UA at GQDs/IL-SPCE was studied in the range of 1.0 to 3.0 mV. In Figure 4.20, the maximum current responses of these three analytes obtained at step potential of 1.5 mV. Consequently, the step potential of 1.5 mV was chosen as the optimal value for further experiments.

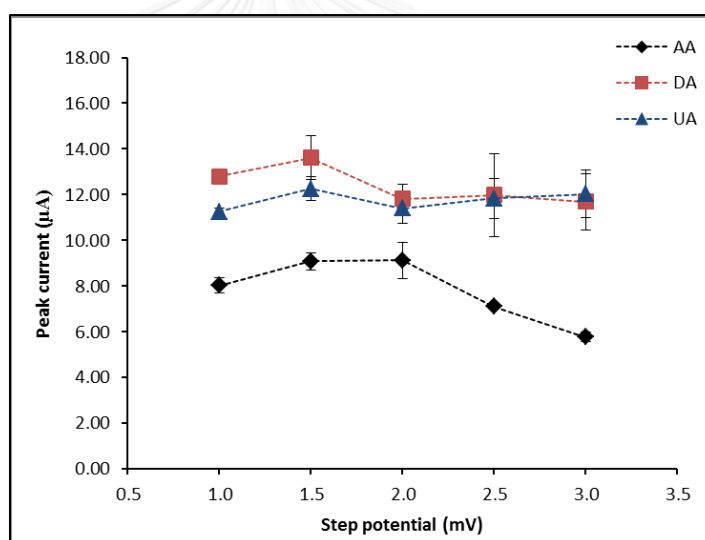


**Figure 4.20** Effect of step potential on the DPV peak currents of 1 mM of AA, 5  $\mu$ M of DA, and 10  $\mu$ M of UA in 0.1 M PBS (pH 4.0) at GQDs/IL-SPCE. Data are shown as the mean  $\pm$  SD and are derived from three replicates.

After that, the effect of pulse amplitude over the range of 20 – 70 mV on the electrocatalytic oxidation of AA, DA, and UA solution is presented in Figure 4.21. The results show that the current responses increased with increasing pulse amplitude value from 20 to 50 mV, but then decreased or slightly increased at pulse amplitude

of more than 50 mV. Therefore, pulse amplitude of 50 mV was selected for the simultaneous measurement of AA, DA, and UA.

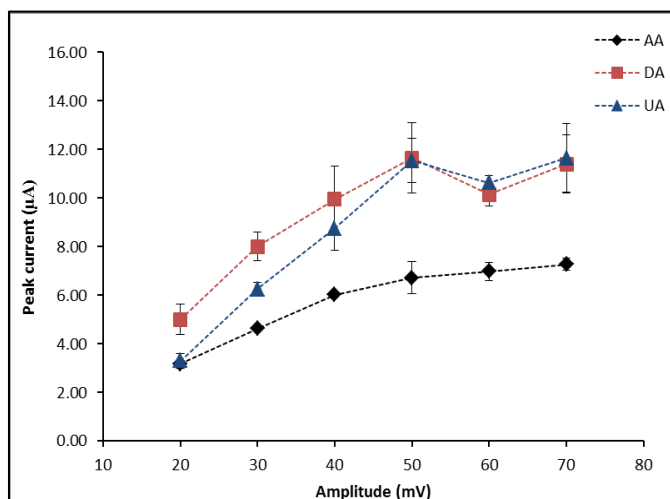


**Figure 4.21** Effect of pulse amplitude on the DPV peak currents of 1 mM of AA, 5  $\mu$ M of DA, and 10  $\mu$ M of UA in 0.1 M PBS (pH 4.0) at GQDs/IL-SPCE. Data are shown as the mean  $\pm$  SD and are derived from three replicates.

Then, the effect of pulse width on the electrochemical response was studied, in the range of 0.2 – 0.6 s. The electrochemical responses of the AA, DA, and UA at various pulse widths on the GQDs/IL-SPCE are shown in Figure 4.22. As the pulse width was increased the anodic peak currents of all three biological compounds increased up to a maximum value at 0.04 s and then decreased with further increases in the pulse width. Subsequently, a pulse width of 0.04 s was selected as an optimal parameter for further study.

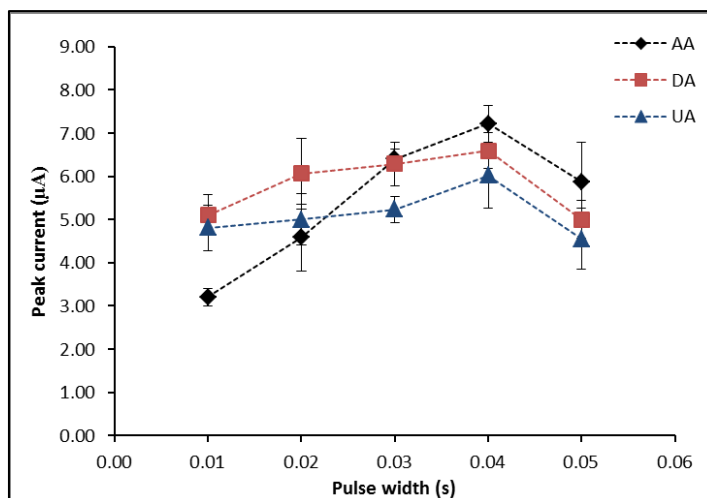


**Figure 4.22** Effect of pulse width on the DPV peak currents of 1 mM of AA, 5  $\mu\text{M}$  of DA, and 10  $\mu\text{M}$  of UA in 0.1 M PBS (pH 4.0) at GQDs/IL-SPCE. Data are shown as the mean  $\pm$  SD and are derived from three replicates.

Finally, the current responses also depended on pulse time. Therefore, the effect of various pulse times on the peak currents of AA, DA, and UA using GQDs/IL-SPCE was investigated. As shown in Figure 4.23, the oxidation peak currents of all analytes increased with increasing the pulse time. Highest current responses for all analytes were obtained and compromised at pulse time of 0.50 s. Thus, pulse time of 0.5 s was used in the next experiments.

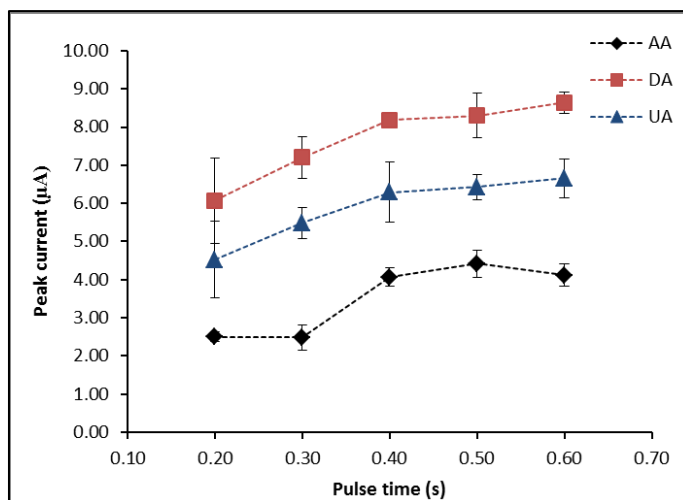


**Figure 4.23** Effect of pulse time on the DPV peak currents of 1 mM of AA, 5  $\mu$ M of DA, and 10  $\mu$ M of UA in 0.1 M PBS (pH 4.0) at GQDs/IL-SPCE. Data are shown as the mean  $\pm$  SD and are derived from three replicates.

The optimized DPV parameters for the simultaneous detection of AA, DA and UA using GQDs/IL-SPCE are summarized in Table 4.1.

**Table 4.1** The optimal DPV parameters for the simultaneous measurement of AA, DA, and UA using GQDs/IL-SPCE

DPV parameters	Examined values	Optimal values
Step potential	1.0 to 3.0 mV	1.5 mV
Pulse amplitude	20 to 70 mV	50 mV
Pulse width	0.01 to 0.05 s	0.04 s
Pulse time	0.2 to 0.6 s	0.5 s

## 4.6 Analytical performance

### 4.6.1 Linearity, LOD and LOQ

The simultaneous determination of AA, DA, and UA was investigated by DPV at QDs/IL-SPCE under optimized conditions. First, the concentration of one analyte was varied, whereas those of the other two compounds were kept constant.

As can be seen in Figure 4.24 – 4.46, the peak potentials of AA, DA, and UA at the GQDs/IL-SPCE were well separated and the anodic peak currents is directly proportional of their concentrations. These results exhibited that the change in the concentration of one of the species has no significant influence on the detection of the other two compounds. Under the optimal conditions, the analytical performance including linear range, LOD and LOQ for the determination of AA, DA, and UA using the proposed method are summarized in Table 4.2. These results show that the DPV method on GQDs/IL-SPCE can be used for the simultaneous determination of AA, DA, and UA.

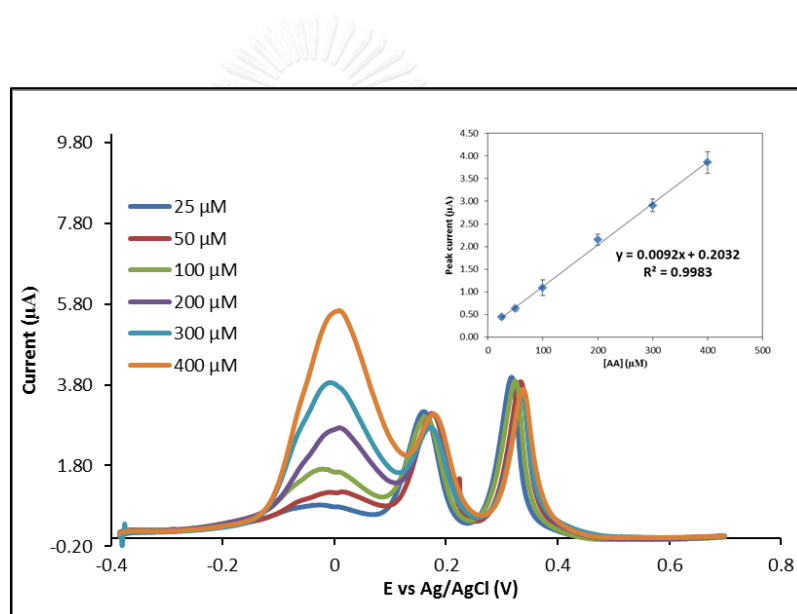


**Figure 4.24** DPV AA in the concentration range of 25-400 μM in the presence of 1 μM DA and 5 μM UA. Inset: Calibration curve of AA by DPV using GQDs/IL-SPCE in the presence of DA and UA. Data are shown as the mean ± SD and are derived from three replicates.

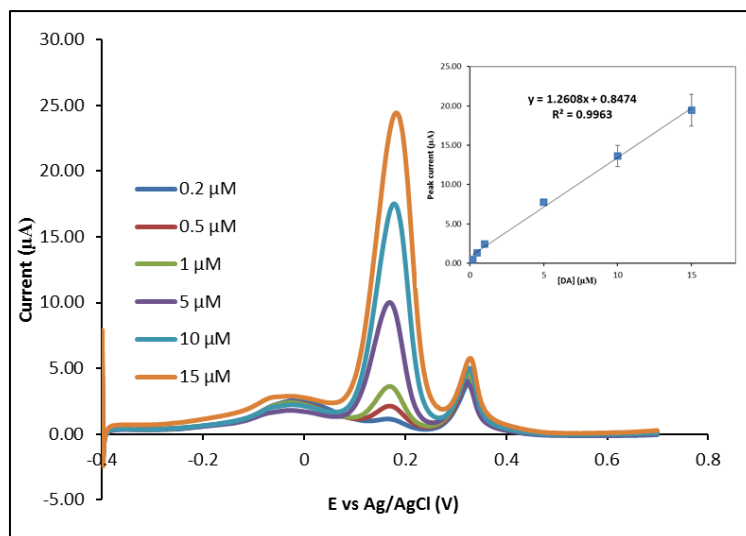


**Figure 4.25** DPV of DA in the concentration range of 0.2-15 μM in the presence of 0.1 mM AA and 5 μM UA. Inset: Calibration curve of DA by DPV using GQDs/IL-SPCE in the presence of AA and UA. Data are shown as the mean ± SD and are derived from three replicates.

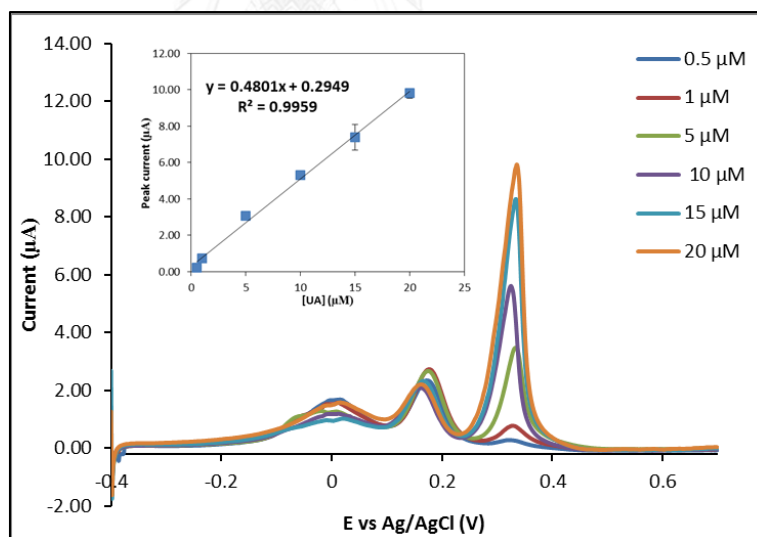


**Figure 4.26** DPV of UA in the concentration range of 0.5-20 μM in the presence of 0.1 mM AA and 1 μM DA. Inset: Calibration curve of UA by DPV using GQDs/IL-SPCE in the presence of AA and DA. Data are shown as the mean ± SD and are derived from three replicates.

**Table 4.2** The analytical performance of determination of AA, DA, and UA by DPV on the GQDs/IL-SPCE in the presence of the other two species.

Analyte	Linear range ( $\mu\text{M}$ )	$R^2$	LOD ( $\mu\text{M}$ )	LOQ ( $\mu\text{M}$ )
AA	25-400	0.9983	6.63	22.13
DA	0.2-15	0.9963	0.06	0.21
UA	0.5-20	0.9959	0.03	0.11

In addition, the simultaneous determination for different concentration of AA, DA, and UA over the range of 25-400  $\mu\text{M}$ , 0.2-6  $\mu\text{M}$  and 0.5-10  $\mu\text{M}$ , respectively, was performed by DPV at GQDs/IL-SPCE. The results are shown in Figure 4.27-4.30; the three oxidation peaks were well peak-to-peak separation and the oxidation peak currents of three analytes increased proportionally to their concentration. The figure of merit for the simultaneous determination of AA, DA, and UA using our proposed method is listed in Table 4.3. Moreover, the performance of the proposed method compared with the other modified electrode report previously is shown in Table 4.4. These results indicated that the developed GQDs/IL/SPCE could be applied to determine trace level of AA, DA and UA in biological fluids with the wide linear range and low detection limits.



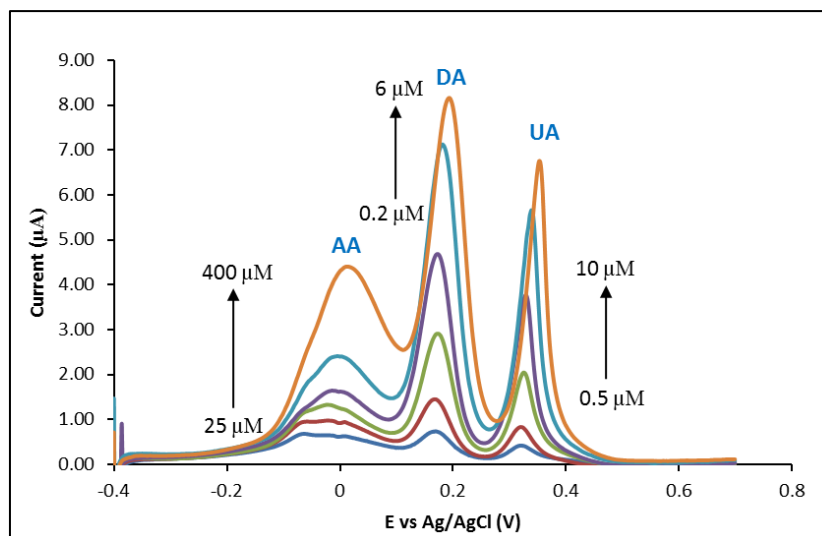


**Figure 4.27** DPV of the simultaneous determination of AA (25-400  $\mu\text{M}$ ), DA (0.2-6  $\mu\text{M}$ ) and UA (0.5-10  $\mu\text{M}$ ) in 0.1 M PBS (pH 4.0) using GQDs/IL-SPCE.

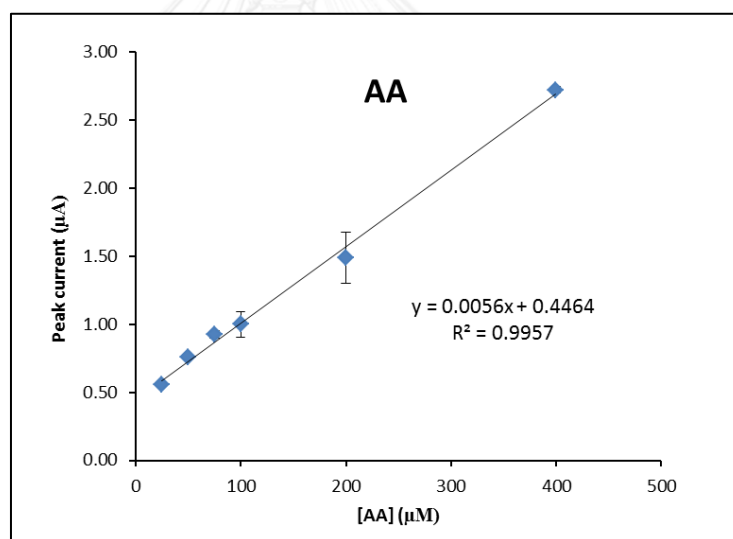


**Figure 4.28** The calibration curve for the simultaneous determination of AA over the concentration range of 25-400  $\mu\text{M}$  in 0.1 M PBS (pH 4.0) by DPV using GQDs/IL-SPCE. Data are shown as the mean  $\pm$  SD and are derived from three replicates.

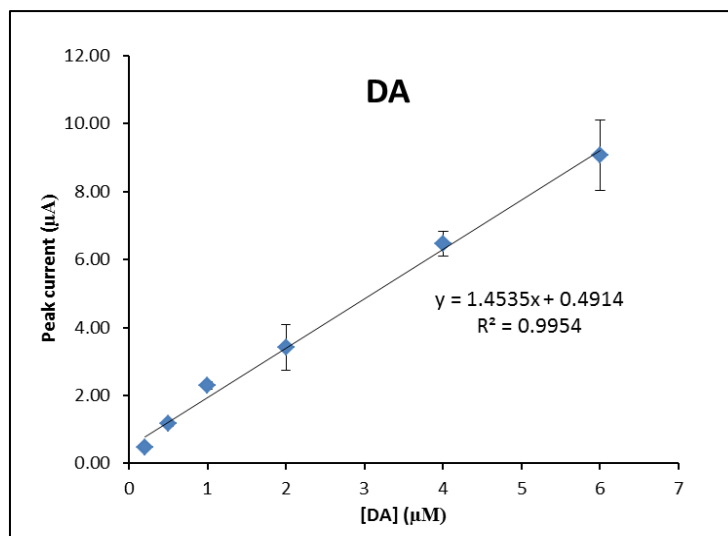


**Figure 4.29** The calibration curve for the simultaneous determination of DA over the concentration range of 0.2-6  $\mu\text{M}$  in 0.1 M PBS (pH 4.0) by DPV using GQDs/IL/SPCE. Data are shown as the mean  $\pm$  SD and are derived from three replicates.

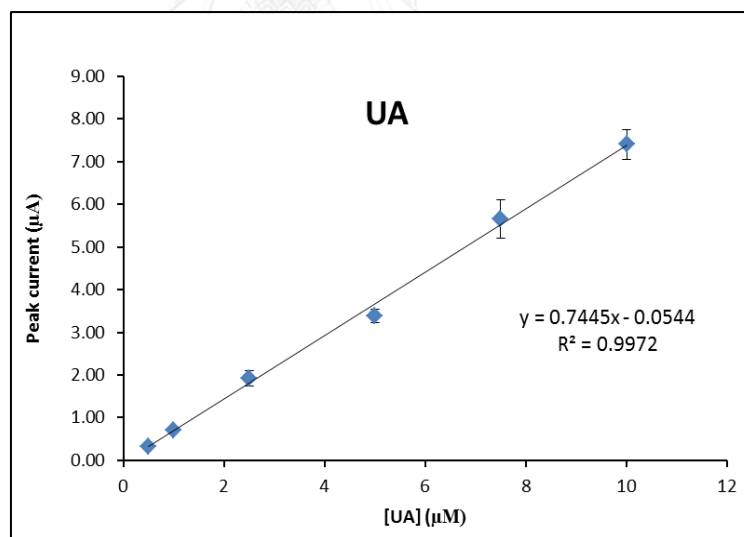


**Figure 4.30** The calibration curve for the simultaneous determination of UA over the concentration range of 0.5-10  $\mu\text{M}$  in 0.1 M PBS (pH 4.0) by DPV using GQDs/IL-SPCE. Data are shown as the mean  $\pm$  SD and are derived from three replicates.

**Table 4.3** The analytical performance of the simultaneous determination of AA, DA and UA by DPV on the GQDs/IL-SPCE

Analyte	Linear range ( $\mu\text{M}$ )	$R^2$	LOD ( $\mu\text{M}$ )	LOQ ( $\mu\text{M}$ )
AA	25-400	0.9957	10.90	36.35
DA	0.2-6	0.9954	0.05	0.18
UA	0.5-10	0.9972	0.02	0.07

**Table 4.4** Comparison of analytical performance of the simultaneous determination of AA, DA and UA by DPV on the GQDs/IL-SPCE with the other modified electrodes in the literature reports.

Electrode	Linear range ( $\mu\text{M}$ )			LOD ( $\mu\text{M}$ )			Reference
	AA	DA	UA	AA	DA	UA	
CILE	2-1,500	50-7,400	7,400	1.00	50	1.00	[16]
SPGNE	4-4,500	0.5-2,000	0.8-2,500	0.95	0.12	0.20	[17]
ERGO/GCE	500-2,000	0.5-60	0.5-60	0.3	0.5	0.5	[30]
Au/RGO/GCE	240-1,500	6.8-410	8.8-53	51	1.4	1.8	[44]
sG/NiO/GCE	150-300	0.44-3.3	2-15	30	0.12	0.46	[33]
MgO/Gr/Ta	5-350	0.1-7	1-70	0.03	0.15	0.12	[34].
GQDs/IL-SPCE	25-400	0.2-15	0.5-20	6.64	0.06	0.03	This work

#### 4.6.2 Reproducibility

In order to evaluate the reproducibility of this method, the response towards the oxidation of 300  $\mu\text{M}$  AA, 5  $\mu\text{M}$  DA, and 5  $\mu\text{M}$  UA in 0.1 M PBS (pH 4.0) was tested by five different GQDs/IL-SPCEs. The results in Figure 4.31 show that the obtained peak responses were not significantly changed in the detection with different sensors. The relative standard deviation (RSD) in peak currents of AA, DA and UA were found to be 4.15%, 3.38%, and 3.47%, respectively. These results exhibit clearly that the modified electrode had good reproducibility.

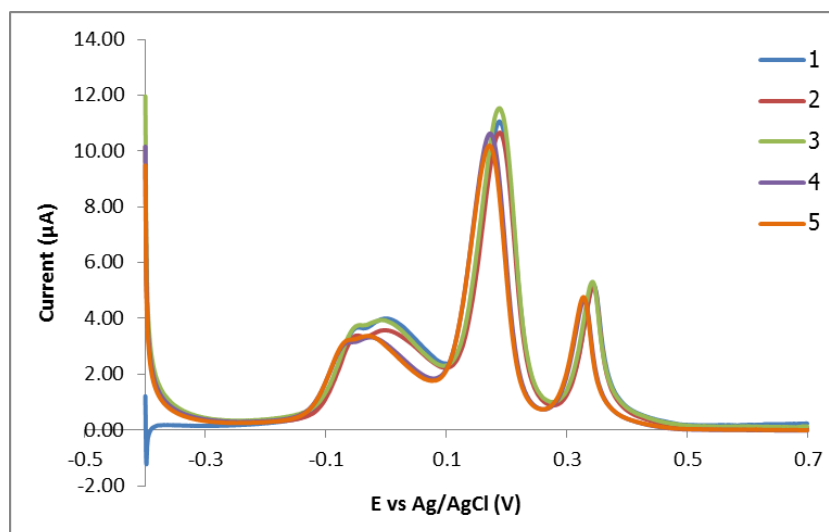


**Figure 4.31** Reproducibility results for DPV determination of 300  $\mu\text{M}$  of AA, 10  $\mu\text{M}$  of DA and 5  $\mu\text{M}$  of UA in 0.1 M PBS (pH 4.0) using 5 different sensors.

#### 4.6.3 Interference study

To investigate the selectivity of the proposed method, the effect of various foreign compounds on the simultaneous determination of 100  $\mu\text{M}$  AA, 10  $\mu\text{M}$  DA, and 5  $\mu\text{M}$  UA was evaluated. The foreign substances including citric acid, glucose, L-cysteine, NaCl, KCl,  $\text{MgSO}_4$ ,  $\text{CaCl}_2$  and  $\text{Zn}(\text{NO}_3)_2$  were selected for this study because they are normally found in biological samples like human serum and urine. Figure 4.32 shows that the 1000  $\mu\text{M}$  of citric acid, glucose, L-cysteine, NaCl, KCl,  $\text{MgSO}_4$ ,  $\text{CaCl}_2$  and  $\text{Zn}(\text{NO}_3)_2$  had no significant interference (signal change < 5%) in the determination of AA, DA and UA [10]. Therefore, our proposed electrode provides highly selective determination of these compounds of interest.

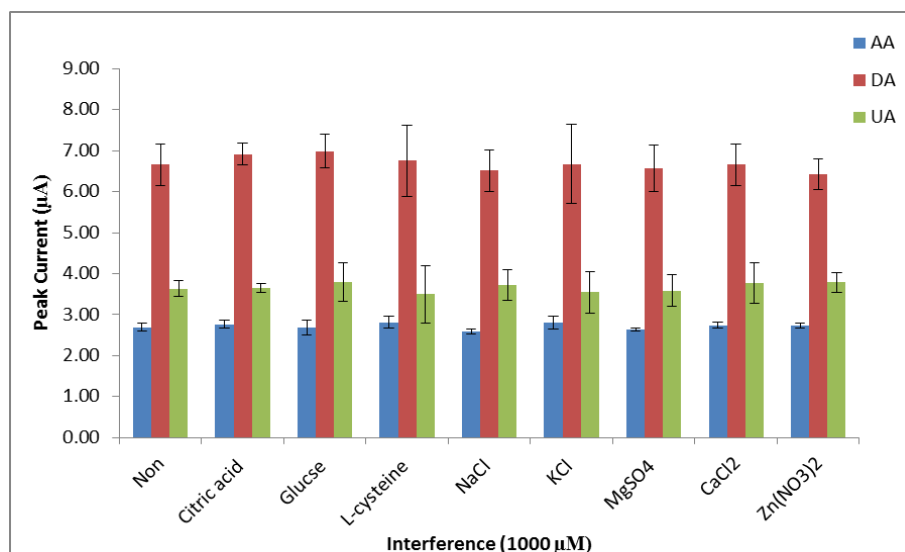


**Figure 4.32** Effect of various foreign substances at 1000  $\mu\text{M}$  on the simultaneous determination of 100  $\mu\text{M}$  of AA, 10  $\mu\text{M}$  of DA, and 5  $\mu\text{M}$  UA in 0.1 M PBS (pH 4.0) by DPV at GQDs/IL-SPCE. Data are shown as the mean  $\pm$  SD and are derived from three replicates.

#### 4.7 Real sample analysis

To verify the performance of developed method, the GQDs/IL-SPCE was applied to the quantitative determination of AA in Vitamin C (Ascee-500<sup>®</sup>) tablets and DA in Dopamine (Domine-250<sup>®</sup>) injection using standard addition method. The amount of AA and DA found in the samples are shown in Table 4.5 with percentage error less than  $\pm 5\%$ . In addition, statistical analysis using student's t-test showed insignificant difference between the results obtained from the method and labeled amounts (at 95% confidence level with  $t_{\text{calculated}}$  below  $t_{\text{critical}}$  at 2.776 and 4 degree of freedom), demonstrating a high accuracy of the proposed method.

**Table 4.5** Determination of ascorbic acid, dopamine and uric acid in vitamin C tablet and dopamine injection (n=3) using our proposed method.

Sample	Labeled amount (mg)	Found amount $\pm$ SD (mg)	% Error
Vitamin C tablet <sup>a</sup>	500	525.00 $\pm$ 0.05	4.60
Dopamine injection <sup>b</sup>	250	241.29 $\pm$ 0.03	3.45

<sup>a</sup> Ascee-500 (B.L. Hua, Thailand)

<sup>b</sup> Domine-250 (Modern Menu, Thailand)

The utilization of the proposed method for the simultaneous determination of AA, DA and UA in real sample was also investigated by direct analysis of human serum without any pretreatment and preparation steps. The DPV responses of these three analytes in human serum are shown in Figure 4.33. It can be seen that the three well-distinguished peaks of AA, DA and UA obtained from the real sample are similar to those of the standard solutions. These confirm that no electrode fouling was observed when measuring real human serum samples. The recovery of the spiked analytes in samples were obtained in the range between 99.04-106.65% (Table 4.6), indicating that the application of the developed method was successfully applied for simultaneously detecting AA, DA and UA in real samples with good recovery and can be used to measure directly without any sample preparation step.

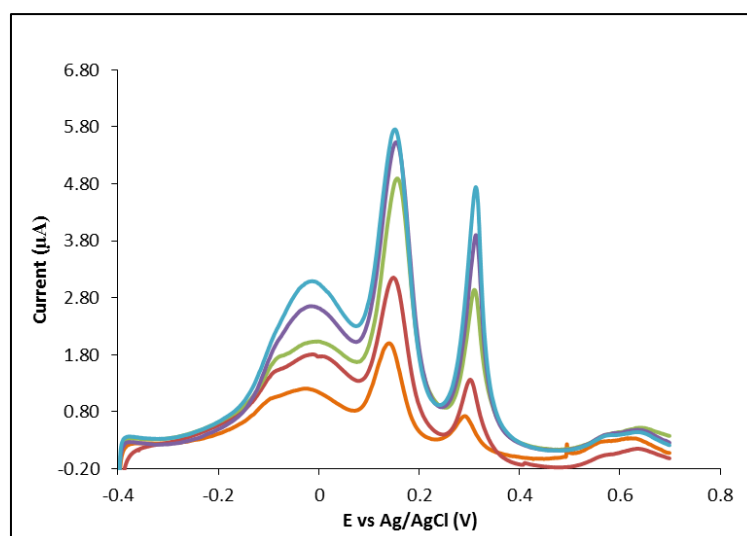


**Figure 4.33** The DPV responses of human serum sample containing different concentrations of added AA, DA and UA in 0.1 M PBS (pH 4.0) on the GQDs/IL-SPCE. Concentration of added three compounds: AA (0, 50, 100, 150, 200  $\mu\text{M}$ ), DA (0, 1, 2, 3, 4  $\mu\text{M}$ ), UA (0, 2, 4, 6, 8  $\mu\text{M}$ ).

**Table 4.6** Determination of ascorbic acid, dopamine and uric acid in human serum sample (n=3) using our proposed method.

Analyte	Spiked concentration	Found concentration $\pm$ SD	% Recovery
	( $\mu\text{M}$ )	( $\mu\text{M}$ )	
AA	0	ND <sup>a</sup>	-
	100	99.04 $\pm$ 5.91	99.04
DA	0	ND <sup>a</sup>	-
	2	2.13 $\pm$ 0.50	106.65
UA	0	ND <sup>a</sup>	-
	1	1.05 $\pm$ 0.33	104.58

ND<sup>a</sup>: Not detectable

## CHAPTER V

### CONCLUSIONS AND SUGGESTION FOR FUTURE WORK

#### 5.1 Conclusions

In this work, a novel electrochemical sensor based on GQDs and IL modified SPCE was developed for the simultaneous determination of AA, DA and UA. The prepared GQDs as electrode modifier were characterized by UV-Vis spectroscopy, FL spectroscopy and TEM. The obtained results confirmed the characteristics of GQDs. The optimized amount of IL and optimized volume of GQDs solution were used to modify the working electrode. The results showed that the modified electrode exhibited remarkable electrocatalytic activity toward the oxidation of AA, DA and UA and also resolved the overlapping anodic peak responses of these three analytes into three well-defined peaks. Furthermore, GQDs/IL-SPCE illustrated high sensitivity, good linear range, low detection limit and good reproducibility for the simultaneous determination of AA, DA and UA. The proposed method was successfully applied to the simultaneous determination of AA, DA and UA in pharmaceutical product and biological sample.

จุฬาลงกรณ์มหาวิทยาลัย  
CHULALONGKORN UNIVERSITY

#### 5.2 SUGGESTION FOR FUTURE WORK

In the future, the GQDs/IL-SPCE has a potential to be applied for the analysis of other sample such as human urine. Moreover, the proposed detection system probably can be developed for the simultaneous determination of AA, DA, UA and tryptophan because these species are usually coexists in biological matrixes.



## REFERENCES

- [1] Pisoschi, A.M., Pop, A., Serban, A.I., and Fafaneata, C. Electrochemical methods for ascorbic acid determination. Electrochimica Acta 121 (2014): 443-460.
- [2] Koshiishi, I. and Imanari, T. Measurement of Ascorbate and Dehydroascorbate Contents in Biological Fluids. Analytical Chemistry 69(2) (1997): 216-220.
- [3] Huot, P., Lévesque, M., and Parent, A. The fate of striatal dopaminergic neurons in Parkinson's disease and Huntington's chorea. Brain 130(1) (2007): 222-232.
- [4] Sulzer, D. How Addictive Drugs Disrupt Presynaptic Dopamine Neurotransmission. Neuron 69(4): 628-649.
- [5] Huang, S.-H., et al. Detection of serum uric acid using the optical polymeric enzyme biochip system. Biosensors and Bioelectronics 19(12) (2004): 1627-1633.
- [6] Schöning, M.J., et al. Amperometric PDMS/glass capillary electrophoresis-based biosensor microchip for catechol and dopamine detection. Sensors and Actuators B: Chemical 108(1-2) (2005): 688-694.
- [7] Yang, J., Sun, C., Wu, X., and Diao, Y.  $\beta$ -CYCLODEXTRIN ENHANCED FLUORIMETRY FOR A DETERMINATION OF ASCORBIC ACID. Analytical Letters 34(8) (2001): 1331-1339.
- [8] Kwon, W., Kim, J.Y., Suh, S., and In, M.K. Simultaneous determination of creatinine and uric acid in urine by liquid chromatography-tandem mass spectrometry with polarity switching electrospray ionization. Forensic Science International 221(1): 57-64.
- [9] Zhao, S., Wang, J., Ye, F., and Liu, Y.-M. Determination of uric acid in human urine and serum by capillary electrophoresis with chemiluminescence detection. Analytical Biochemistry 378(2) (2008): 127-131.
- [10] Ouyang, X., Luo, L., Ding, Y., Liu, B., Xu, D., and Huang, A. Simultaneous determination of uric acid, dopamine and ascorbic acid based on

- poly(bromocresol green) modified glassy carbon electrode. Journal of Electroanalytical Chemistry 748 (2015): 1-7.
- [11] Roy, P.R., Okajima, T., and Ohsaka, T. Simultaneous electroanalysis of dopamine and ascorbic acid using poly (N,N-dimethylaniline)-modified electrodes. Bioelectrochemistry 59(1-2) (2003): 11-19.
- [12] Atta, N.F., Ali, S.M., El-Ads, E.H., and Galal, A. Nano-perovskite carbon paste composite electrode for the simultaneous determination of dopamine, ascorbic acid and uric acid. Electrochimica Acta 128 (2014): 16-24.
- [13] Li, M., Guo, W., Li, H., Dai, W., and Yang, B. Electrochemical biosensor based on one-dimensional MgO nanostructures for the simultaneous determination of ascorbic acid, dopamine, and uric acid. Sensors and Actuators B: Chemical 204 (2014): 629-636.
- [14] Li, H., et al. An electrochemical sensor for simultaneous determination of ascorbic acid, dopamine, uric acid and tryptophan based on MWNTs bridged mesocellular graphene foam nanocomposite. Talanta 127 (2014): 255-261.
- [15] Cai, W., Lai, J., Lai, T., Xie, H., and Ye, J. Controlled Functionalization of Flexible Graphene Fibers for the Simultaneous Determination of Ascorbic Acid, Dopamine and Uric Acid. Sensors and Actuators B: Chemical.
- [16] Safavi, A., Maleki, N., Moradlou, O., and Tajabadi, F. Simultaneous determination of dopamine, ascorbic acid, and uric acid using carbon ionic liquid electrode. Analytical Biochemistry 359(2) (2006): 224-229.
- [17] Ping, J., Wu, J., Wang, Y., and Ying, Y. Simultaneous determination of ascorbic acid, dopamine and uric acid using high-performance screen-printed graphene electrode. Biosensors and Bioelectronics 34(1) (2012): 70-76.
- [18] Noyrod, P., Chailapakul, O., Wonsawat, W., and Chuanuwatanakul, S. The simultaneous determination of isoproturon and carbendazim pesticides by single drop analysis using a graphene-based electrochemical sensor. Journal of Electroanalytical Chemistry 719 (2014): 54-59.
- [19] Bacon, M., Bradley, S.J., and Nann, T. Graphene Quantum Dots. Particle & Particle Systems Characterization 31(4) (2014): 415-428.

- [20] Zhang, Z., Zhang, J., Chen, N., and Qu, L. Graphene quantum dots: an emerging material for energy-related applications and beyond. Energy & Environmental Science 5(10) (2012): 8869-8890.
- [21] Sajid, M., Nazal, M.K., Mansha, M., Alsharaa, A., Jillani, S.M.S., and Basheer, C. Chemically modified electrodes for electrochemical detection of dopamine in presence of uric acid and ascorbic acid: a review. TrAC Trends in Analytical Chemistry.
- [22] Lakshmi, D., Whitcombe, M.J., Davis, F., Sharma, P.S., and Prasad, B.B. Electrochemical Detection of Uric Acid in Mixed and Clinical Samples: A Review. Electroanalysis 23(2) (2011): 305-320.
- [23] Bard, A.J. and Faulkner, L.R. Electrochemical Methods: Fundamentals and Applications. Wiley, 2000.
- [24] Goldsmith, J.G. Modern Analytical Chemistry, 1st Edition (Harvey, David). Journal of Chemical Education 77(6) (2000): 705.
- [25] Couto, R.A.S., Lima, J.L.F.C., and Quinaz, M.B. Recent developments, characteristics and potential applications of screen-printed electrodes in pharmaceutical and biological analysis. Talanta.
- [26] Ionic Liquids [Online]. Available from: <http://www.sigmaaldrich.com/technical-documents/articles/chemfiles/ionic-liquids0.html> [23 November]
- [27] Dong, Y., et al. Blue luminescent graphene quantum dots and graphene oxide prepared by tuning the carbonization degree of citric acid. Carbon 50(12) (2012): 4738-4743.
- [28] Roushani, M. and Abdi, Z. Novel electrochemical sensor based on graphene quantum dots/riboflavin nanocomposite for the detection of persulfate. Sensors and Actuators B: Chemical 201 (2014): 503-510.
- [29] Afraz, A., Rafati, A.A., and Najafi, M. Optimization of modified carbon paste electrode with multiwalled carbon nanotube/ionic liquid/cauliflower-like gold nanostructures for simultaneous determination of ascorbic acid, dopamine and uric acid. Materials Science and Engineering: C 44 (2014): 58-68.
- [30] Yang, L., Liu, D., Huang, J., and You, T. Simultaneous determination of dopamine, ascorbic acid and uric acid at electrochemically reduced graphene

- oxide modified electrode. Sensors and Actuators B: Chemical 193 (2014): 166-172.
- [31] Wang, C., Xu, P., and Zhuo, K. Ionic Liquid Functionalized Graphene-Based Electrochemical Biosensor for Simultaneous Determination of Dopamine and Uric Acid in the Presence of Ascorbic Acid. Electroanalysis 26(1) (2014): 191-198.
- [32] Hu, S., et al. Reduced graphene oxide-carbon dots composite as an enhanced material for electrochemical determination of dopamine. Electrochimica Acta 130 (2014): 805-809.
- [33] Nancy, T.E.M. and Kumary, V.A. Synergistic electrocatalytic effect of graphene/nickel hydroxide composite for the simultaneous electrochemical determination of ascorbic acid, dopamine and uric acid. Electrochimica Acta 133 (2014): 233-240.
- [34] Zhao, L., et al. MgO nanobelt-modified graphene-tantalum wire electrode for the simultaneous determination of ascorbic acid, dopamine and uric acid. Electrochimica Acta 168 (2015): 191-198.
- [35] Ju, J. and Chen, W. Synthesis of highly fluorescent nitrogen-doped graphene quantum dots for sensitive, label-free detection of Fe (III) in aqueous media. Biosensors and Bioelectronics 58 (2014): 219-225.
- [36] Amjadi, M., Manzoori, J.L., and Hallaj, T. Chemiluminescence of graphene quantum dots and its application to the determination of uric acid. Journal of Luminescence 153 (2014): 73-78.
- [37] Liu, Y., Wang, D., Huang, J., Hou, H., and You, T. Highly sensitive composite electrode based on electrospun carbon nanofibers and ionic liquid. Electrochemistry Communications 12(8) (2010): 1108-1111.
- [38] Zhao, J., Zhao, L., Lan, C., and Zhao, S. Graphene quantum dots as effective probes for label-free fluorescence detection of dopamine. Sensors and Actuators B: Chemical.
- [39] Lim, C.S., Hola, K., Ambrosi, A., Zboril, R., and Pumera, M. Graphene and carbon quantum dots electrochemistry. Electrochemistry Communications 52 (2015): 75-79.

- [40] Maleki, N., Safavi, A., and Tajabadi, F. High-Performance Carbon Composite Electrode Based on an Ionic Liquid as a Binder. Analytical Chemistry 78(11) (2006): 3820-3826.
- [41] Sun, W., Yang, M., and Jiao, K. Electrocatalytic oxidation of dopamine at an ionic liquid modified carbon paste electrode and its analytical application. Analytical and Bioanalytical Chemistry 389(4) (2007): 1283-1291.
- [42] Razmi, H. and Mohammad-Rezaei, R. Graphene quantum dots as a new substrate for immobilization and direct electrochemistry of glucose oxidase: Application to sensitive glucose determination. Biosensors and Bioelectronics 41 (2013): 498-504.
- [43] Pandurangachar, M., Swamy, B.E.K., Chandra, U., Gilbert, O., and Sherigara, B.S. Simultaneous determination of dopamine, ascorbic acid and uric acid at poly(Patton and Reeder's) modified carbon paste electrode. International Journal of Electrochemical Science 4(5) (2009): 672-683.
- [44] Wang, C., et al. A facile electrochemical sensor based on reduced graphene oxide and Au nanoplates modified glassy carbon electrode for simultaneous detection of ascorbic acid, dopamine and uric acid. Sensors and Actuators B: Chemical 204 (2014): 302-309.



APPENDIX

จุฬาลงกรณ์มหาวิทยาลัย  
CHULALONGKORN UNIVERSITY

## APPENDIX A

## Optimization of modified electrode and the DPV conditions

## 1. Optimization of modified electrode

The influence of pH on the anodic peak currents of AA, DA and UA

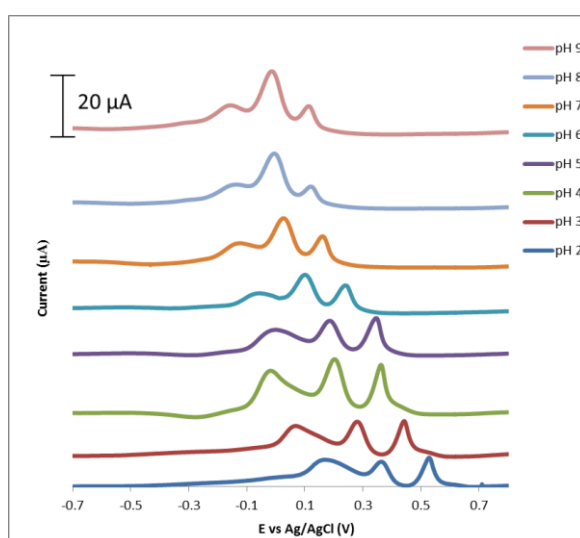


**Figure A1** Effect of pH on the DPV responses of 1 mM AA, 5 μM DA and 10 μM UA in 0.1 M PBS (pH 4.0) at GQDs/IL-SPCE.

## 2. Optimization of the DPV conditions

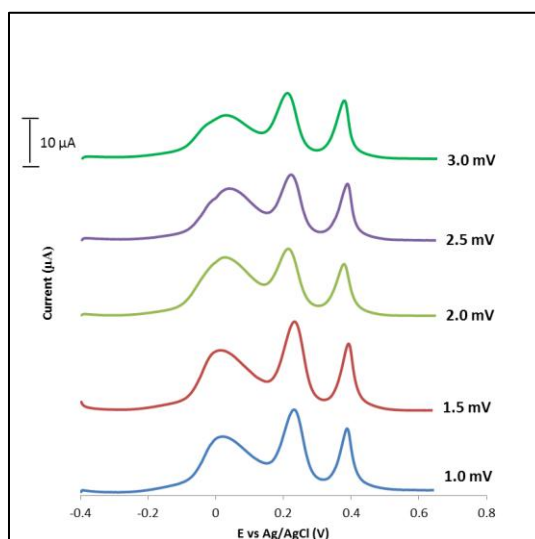


**Figure A2** Effect of step potential on the DPV responses of 1 mM AA, 5 μM DA and 10 μM UA in 0.1 M PBS (pH 4.0) at GQDs/IL-SPCE.

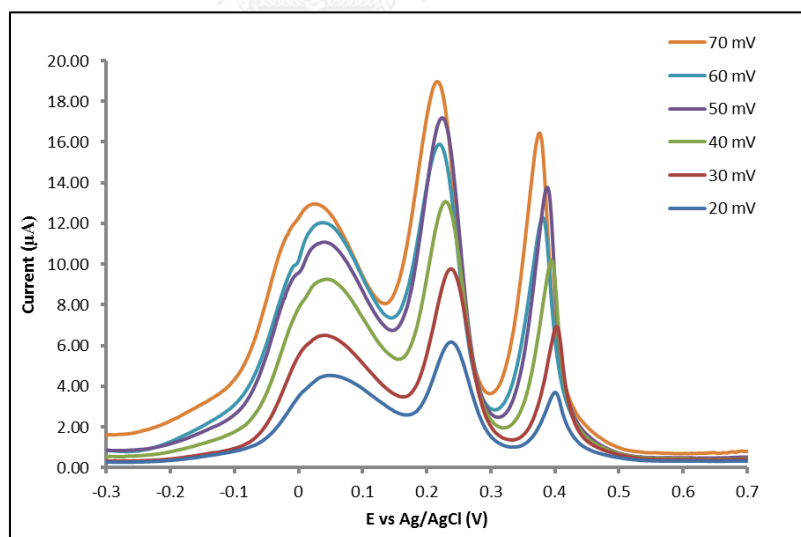


**Figure A3** Effect of pulse amplitude on the DPV responses of 1 mM AA, 5 μM DA and 10 μM UA in 0.1 M PBS (pH 4.0) at GQDs/IL-SPCE.



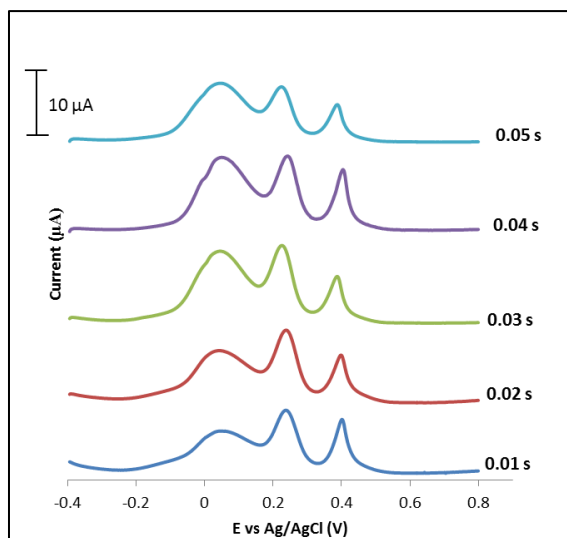


**Figure A4** Effect of pulse width on the DPV responses of 1 mM AA, 5  $\mu\text{M}$  DA and 10  $\mu\text{M}$  UA in 0.1 M PBS (pH 4.0) at GQDs/IL-SPCE.

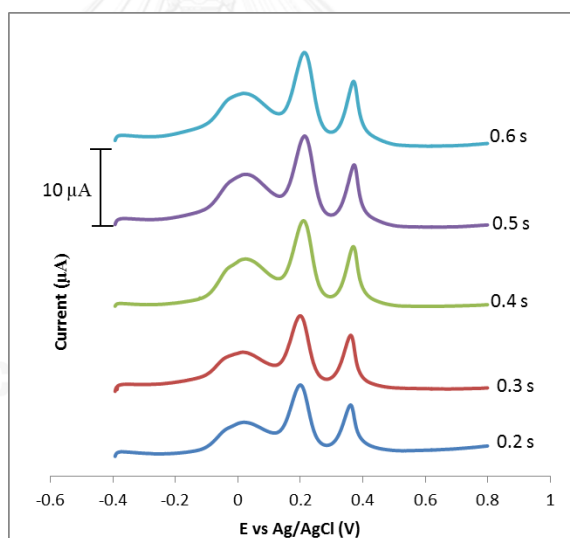


**Figure A5** Effect of pulse time on the DPV responses of 1 mM AA, 5  $\mu\text{M}$  DA and 10  $\mu\text{M}$  UA in 0.1 M PBS (pH 4.0) at GQDs/IL-SPCE.

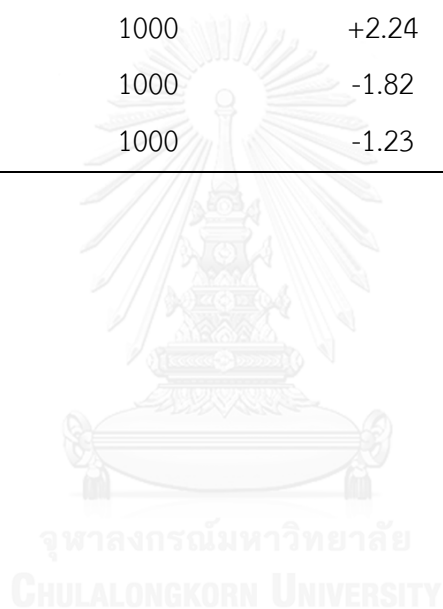
**APPENDIX B**  
**Reproducibility and Interference Study**

**Table B1** The anodic peak currents of 300  $\mu\text{M}$  AA, 5  $\mu\text{M}$  DA, and 5  $\mu\text{M}$  UA in 0.1 M PBS (pH 4.0) using 5 different sensors.

Number of electrode	Current ( $\mu\text{A}$ )		
	AA	DA	UA
1	2.43	9.37	4.41
2	2.30	9.11	4.45
3	2.52	9.89	4.51
4	2.24	9.35	4.11
5	2.35	8.96	4.22
Mean	2.37	9.34	4.34
SD	0.10	0.32	0.15
%RSD	4.15	3.38	3.47

**Table B2** The influences of some metal ions and important biological substances on the peak currents of 100  $\mu\text{M}$  of AA, 10  $\mu\text{M}$  of DA, and 5  $\mu\text{M}$  UA in 0.1 M PBS (pH 4.0).

Potential Interfering substance	Concentration ( $\mu\text{M}$ )	Signal change (%)		
		AA	DA	UA
Citric acid	1000	-2.37	-3.93	-0.05
Glucose	1000	+0.46	-4.97	-4.23
L-cysteine	1000	-4.15	-1.45	+3.89
NaCl	1000	+4.12	+2.04	-2.36
KCl	1000	-4.15	-0.33	+2.54
MgSO <sub>4</sub>	1000	+2.24	+1.29	+1.45
CaCl <sub>2</sub>	1000	-1.82	+0.02	-3.71
Zn(NO <sub>3</sub> ) <sub>2</sub>	1000	-1.23	+3.40	-4.23



## APPENDIX C

### Precision and Accuracy

**Table C1** The acceptable reproducibility, the data from AOAC official method of analysis (2012).

Analyte concentration	% RSD
100%	2
10%	3
1%	4
0.1%	6
0.01%	8
10 µg/g (ppm)	11
1 µg/g	16
10 µg/kg (ppb)	32

**Table C2** Accuracy consisted from AOAC AOAC official method of analysis (2012).

Analyte concentration	% Recovery
100%	98-101
10%	95-102
1%	92-105
0.10%	90-108
0.01%100 ppm	85-110
10 µg/g (ppm)	80-115
1 µg/g	75-120
10 µg/kg (ppb)	70-125

## VITA

Ms. Kanjana Kunpatee was born on May 20, 1991 in Yasothon, Thailand. She received her Bachelor's degree of Science (Chemistry) with first class honor from Ubon Ratchathani University, Ubon Ratchathani, Thailand in 2012. After that, she accordingly becomes a Master's degree of Science (Analytical Chemistry) of academic year 2015 from Chulalongkorn University.

### Proceedings:

Kanjana Kunpatee, Suchada Chuanuwatanakul "Method development for determination of ascorbic acid, dopamine and uric acid using graphene quantum dots/ionic liquid modified screen-printed carbon electrode" Proceedings of The 5th Asian Symposium on Advanced Materials: Chemistry, Physics & Biomedicine of Functional and Novel Materials (ASAM-5), Pusan National University, Busan, Korea, November 1-4, 2015, pp 185-189.

### Publication:

Anchalee Samphao, Kanjana Kunpatee, Sanchai Prayoonpokarach, Jatuporn Wittayakun, **L**ubomír Švorc, Dalibor M. Stankovic, Kristina Zagar, Miran Ceh and Kurt Kalcher, An ethanol biosensor based on simple immobilization of alcohol dehydrogenase on Fe<sub>3</sub>O<sub>4</sub>@Au nanoparticles, *Electroanalysis*, 27 (2015) 1-10.